Geologica Acta, Vol.7, Nos 1-2, March-June 2009, 11-34
DOI: 10.1344/105.000000279
Available online at www.geologica-acta.com

Late Maastrichtian-Early Paleocene sea level and climate changes in the Antioch Church Core (Alabama, Gulf of Mexico margin, USA): A multi-proxy approach

PETER SCHULTE [1] **and ROBERT P. SPEIJER** [2]

[1] **GeoZentrum Nordbayern, Universität Erlangen**
Schlossgarten 5, D-91054 Erlangen, Germany. E-mail: schulte@geol.uni-erlangen.de

[2] **Department of Earth and Environmental Sciences, K.U.Leuven**
Celestijnenlaan 200E, B-3001 Leuven, Belgium. E-mail: robert.speijer@ees.kuleuven.be

ABSTRACT

The Antioch Church core from central Alabama, spanning the Cretaceous-Paleogene (K-P) boundary, was investigated by a multi-proxy approach to study paleoenvironmental and sea level changes within the well-constrained sequence stratigraphic setting of the Gulf of Mexico margin. The Antioch Church core comprises the Maastrichtian calcareous nannoplankton Zone CC25 and the Danian Zones NP1 to NP4 corresponding to the Maastrichtian planktonic foraminifera Zones CF3 and the Danian Zones P1a to P2. Facies shifts from a Maastrichtian siliciclastic to a mixed siliciclastic-carbonate depositional system during the late Danian. Sedimentary proxies indicate that depositional settings changed between littoral (foreshore) and inner and middle neritic (offshore transition zone). Four sedimentary sequences, each encompassing LST, TST, and HST were identified. Estimated water depths by using benthic foraminiferal assemblages were not exceeding 20-40 m for the Maastrichtian and 0-40 m for the Danian sequences. The succession of facies shifts within systems tracts can be very well disentangled by major and trace element data as well as by various element ratios including Zr/Rb, (Zr+Rb)/Ca, and Sr/Ca. By applying element stratigraphy, the ambiguities of the natural gamma ray log –with peaks associated either with maximum flooding surfaces or with silty lag deposits ("placer silts") during the late regressive HST– are resolved. In addition, the Zr/Rb ratio provides a good proxy for monitoring grain size distribution and sorting effects. According to the Antioch Church core data, the K-P boundary is associated with a sandstone event bed that includes ejecta spherules from the Chicxulub impact. However, the genesis of the K-P event bed, whether lowstand, tempestite- or tsunami-related, cannot be resolved from this core. In terms of clay mineralogy, the studied interval is characterized by a steady increase in smectite that parallels a decrease in kaolinite with the latter disappearing about two My after the K-P boundary during Biozone NP2. This change in the clay mineral assemblage, which is almost independent of lithology, may suggest a long-term shift from stable, tropical warm and humid climates during the latest Maastrichtian to warm climate with alternating humid and arid seasons in the middle Danian.

KEYWORDS | **K-T boundary. Cretaceous-Paleogene boundary. Paleoclimate. Sequence stratigraphy. Benthic Foraminifera. Clay Mineralogy.**

INTRODUCTION

The succession of Maastrichtian to Paleocene strata on the Alabama coastal plain has played a central role in the development of sequence stratigraphic concepts due to the outstanding combination of outcrop, core, and seismic data on the slowly subsiding passive margin. Consequently, a well-constrained high-resolution sequence stratigraphic framework exists (Baum and Vail, 1988; Donovan et al., 1988; Savrda, 1991; Mancini and Tew, 1993), which also served as a reference for the lower Paleogene in the sequence cycle chart of Haq et al. (1988). These studies reveal a striking difference between upper Cretaceous and lower Paleogene sequences – with long-term cycles in the Maastrichtian and frequent, short-term cycles in the Danian. However, a mixed siliciclastic-carbonate depositional system was established during the Danian, which makes recognition of sequence stratigraphic surfaces difficult due to varying rates of biological and carbonate productivity versus siliciclastic influx (Mancini and Tew, 1997). Therefore, constraining ages of sequence boundaries as well as magnitudes of sea level change is complicated (Olsson and Liu, 1993).

The presence of channeled sandstones at the Cretaceous-Paleogene (K-P) boundary has further contributed to the uncertainties of determining late Cretaceous-early Paleogene sea-level changes. These sandstones have traditionally been considered as bar sands or incised valley fill deposits genetically linked to a sea-level lowstand (e.g., Baum and Vail, 1988; Donovan et al., 1988; Mancini and Tew, 1993). Alternatively, these sandstones have been interpreted as tempestite or tsunami event deposit associated with the Chicxulub impact (e.g., Olsson et al., 1996; Smit et al., 1996).

The Antioch Church core from central Alabama provides a more expanded late Maastrichtian and Danian succession than the adjacent well-known Braggs and Mussel Creek K-P outcrop sections (Jones et al., 1987; Donovan et al., 1988; Baum and Vail, 1988; Zachos et al., 1989; Savrda, 1993). Moreover, weathering does not bias its geologic record. With our multi-proxy approach incorporating sediment petrology, mineralogy, geochemistry, and foraminifera and by making use of the previously established sequence stratigraphic architecture for the Gulf of Mexico Margin (Donovan et al., 1988; Baum and Vail, 1988), we investigate late Cretaceous vs. early Paleogene environmental changes. Specifically, we intend to answer the following questions:

a) Do systematic changes occur when comparing late Maastrichtian and early Danian sequences via petrographic, mineralogical, and geochemical proxy data?

b) Are the water depth changes given by previous studies for central Alabama (30-80 m water depth; Baum and Vail, 1988; Olsson et al., 1996) in line with foraminiferal data?

c) Is it possible to derive relevant stratigraphic patterns from geochemical facies analysis on a sub-systems tract scale?

d) Do clay mineral assemblages show climatically relevant variations?

In addition, the K-P boundary interval in the Antioch Church core may provide further constraints on the genesis of the K-P boundary sandstone deposit and possible links to the Chicxulub impact on the Yucatan carbonate platform, southern Mexico.

GEOLOGICAL SETTING

The Antioch Church Core was cored in South-central Alabama, about 140 m north of Alabama Route 263 and 5 km northwest of Greenville in Lowndes County (Fig. 1). The core site is located in a downdip setting about 7.4 km northeast and 3.6 km east of the well known Braggs and Mussel Creek K-P boundary localities, respectively, and was drilled in front of the abandoned building of the Baptist "Antioch Church."

Generally, the late Cretaceous to early Paleocene strata of southern and central Alabama constitute a seaward-dipping wedge of sedimentary rocks that reflects the infilling of a slowly, but differentially subsiding depositional basin on the passive southern margin of the North American continent (Fig. 1; Sohl et al., 1991; Mancini and Tew, 1993). Lateral lithofacies changes from west to east indicate that depositional conditions in southwest Alabama during this period were associated with deltaic and marginal marine sediment accumulation. Sedimentation in southeast and south-central Alabama was controlled by the presence of a persistent Paleocene carbonate platform that formed over Paleozoic basement rocks and was little affected by salt tectonics. During the early Paleocene, a delta developed in Mississippi and in western Alabama, resulting in increased siliciclastic sedimentation (Mancini and Tew, 1993). Facies shifts on the Alabama paleoshelf from siliciclastic-dominated deposition during the late Maastrichtian to a siliciclastic-carbonate depositional system in the Danian.

For the about 84 m thick interval from the latest Maastrichtian to the late Danian, which is recorded in the sediments of the Antioch Church core, Baum and Vail (1988), Mancini and Tew (1993), and Mancini et al. (1996), delineated a distinct succession of four unconformities that divide the lower and upper part of the Midway Group into distinct depositional sequences (Fig. 1). These unconformity-bound sedimentary sequences are now

exposed along the SSE-NWW-trending outcrop belt of Cretaceous and Paleocene units in the Gulf of Mexico coastal plain of Alabama, though local derivations exist in thickness and extent of individual units (see Mancini and Tew, 1993 for details on regional paleogeographic aspects). These depositional sequences are outlined in the following and exemplarily depicted in Fig. 1.

Sequence 1: The upper Maastrichtian UZGC-5.0 ("Upper Zuni, Gulf Coast Cycle") sequence is composed of the Prairie Bluff Formation (Fm) and represents late highstand or regressive deposits (Mancini et al., 1996).

Sequence 2: The lower Danian TAGC-1.1 ("Tejas A, Gulf Coast Cycle") sequence comprises the Clayton Basal Sands and the overlying Pine Barren Member of the Clayton Fm (Donovan et al., 1988; Baum and Vail, 1988; Mancini and Tew, 1993): The lower boundary of this sequence in the Gulf Coast Plain area is considered as type-1 unconformity, with the Clayton Basal Sands considered as incised valley fill deposits that developed when sea-level fell below the shelf break. The overlying Pine Barren Member includes a prominent glauconitic maximum flooding in South-central Alabama that separates the retrograding, transgressive sandy limestones below from the prograding highstand marls and silty/sandy mudstones above.

Sequence 3: The early Danian (TAGC-1.2) includes the prominent *Turritella* Rock, which is interpreted as shelf-margin systems tract, and the McBryde Limestone Member of the Clayton Fm (Mancini and Tew, 1993).

Sequence 4: The third Danian (TAGC-1.3) sequence comprises the upper part of the McBryde Limestone Member of the Clayton Fm and the lower part of the Porters Creek Fm (Mancini and Tew, 1993).

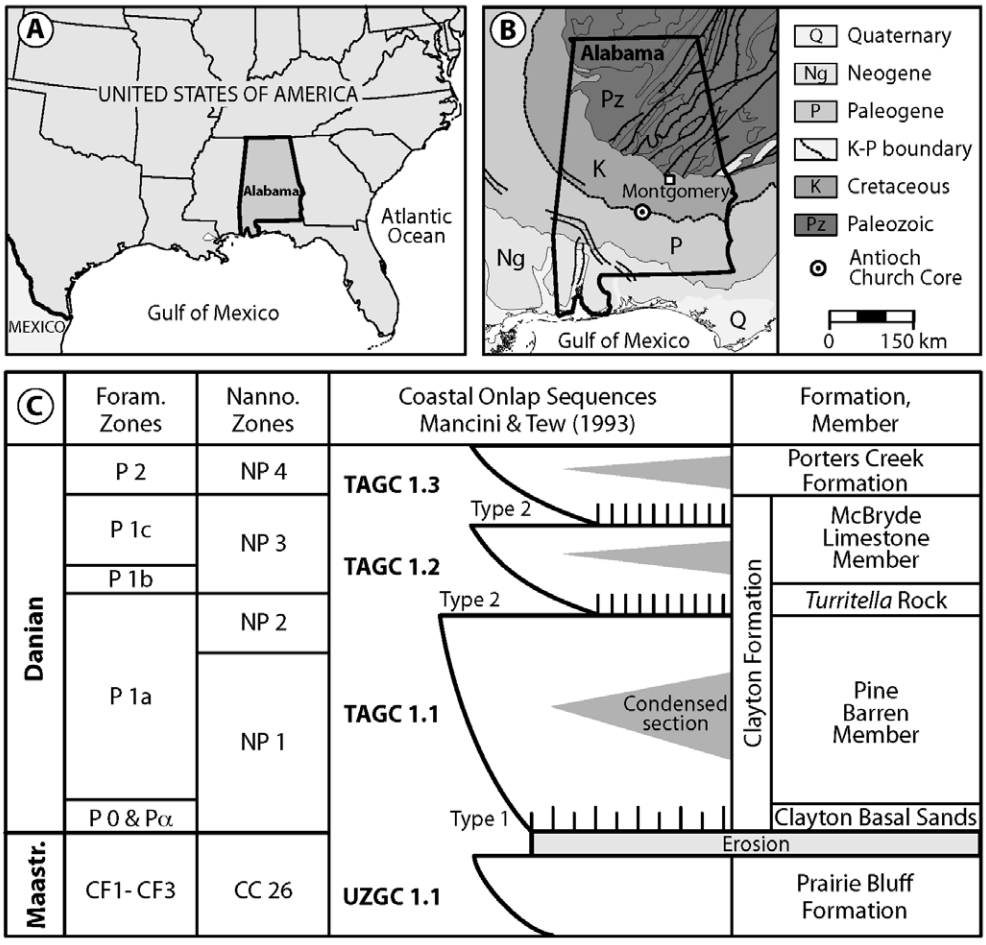

FIGURE 1 | **A) Location of Alabama at the Gulf of Mexico Coastal Plain. B) Schematic geologic map of Alabama showing the Cretaceous-Paleogene outcrop belt and the location of the Antioch Church Core. C) Biostratigraphy and third-order coastal onlap cycles recognized for Maastrichtian-Paleocene strata in South-Central Alabama (modified from Mancini and Tew, 1993).**

METHODOLOGY

Two hundred thirty five closely-spaced samples labeled AC (Antioch Church) were taken during a visit at Princeton University together with Wolfgang Stinnesbeck and Gerald Baum in 2001. Optical microscopy of about 80 resin-stained thin sections was performed to assess the textural and mineralogical properties. Petrographic composition was analyzed by point counting (100 points) on each thin section to develop grain size and quantities of grains, cement, and porosity.

For nannofossil biostratigraphy, sample material was ultrasonically cleaned in a weak ammonium solution for 3 min. The resulting suspension was allowed to settle for 3 min and the water decanted. The deposit was then again brought into suspension and a few drops spread over a graphitic scanning electron microscope (SEM) stub. After drying and coating with gold, the stub was observed in a SEM at 2.5 K magnification. For qualitative and quantitative foraminiferal analysis, samples were disintegrated and sieved. The size fraction >125 μm was used for estimating planktic/benthic ratios and for semi-quantitative benthic foraminiferal analysis.

Selected major and trace elements (CaO_2, Fe_2O_3, TiO_2, K_2O, Cr, Ni, Cu, Zn, As, Rb, Sr, Y, Zr, Ba, La, Ce, Nb, and Pb) were analyzed from bulk powder samples (5 g) by energy-dispersive X-ray fluorescence spectrometry (EDS) with a SPECTRACE 5000 X-ray analyzer at the Institute for Mineralogy and Geochemistry, University of Karlsruhe (Kramar, 1997). Analytical error is generally lower than 10% relative. The element-specific detection limits are given in Table 1. Further major elements were analyzed by wavelength-dispersive X-ray fluorescence spectrometry (WDS) also at the Institute for Mineralogy and Geochemistry, University of Karlsruhe, with a SRS 303 AS XRF. For these analyses, fused glass discs were prepared from a mixture of 1 g ignited powder of each sample and 4 g of SPECTROMELT.

Total organic carbon (TOC) content analysis was performed with a ROCK EVAL 6 pyrolizer at the Geological Institute of Houston, Texas, and at the University of Neuchâtel, Switzerland (Langford and Blanc-Valleron, 1990). The obtained values were compared with a standard reference sample. Analytical precision for a standard is 0.003% and reproducibility is 0.02% for the insoluble residue.

Clay mineralogy was analyzed by X-ray diffractometry (XRD) at the Geological Institute of the University of Neuchâtel, Switzerland, with a SCINTAG XRD 2000 diffractometer and Cu-k⟨- radiation after methods given in Adatte et al. (2002). Diffractograms were evaluated with the MacDIFF software (Petschick et al., 1996). The semi-quantitative estimation of the relative abundance of the clay minerals was conducted by using the ratios of the weighted peak areas of smectite (weighting factor '1'), chlorite ('2'), illite ('4'), and kaolinite ('2') from glycolated specimen of the <2 μm fraction (see Fig. A1 in Appendix at www.geologica-acta.com).

LITHOLOGY, PETROLOGY AND DEPOSITIONAL SEQUENCES

Centimeter-scale core and petrographic observations on the lithologic and faunal composition, sedimentary texture and structure were used first to interpret lithofacies and associated depositional systems of the Antioch Church core. These facies and associated environments of individual sequences, complemented by the benthic foraminifera and geochemical data in the next sections, reveal diagnostic information on processes controlling sequence formation.

Prairie Bluff Formation

The Prairie Bluff Fm in the Antioch Church core consists of silty-sandy micaceous mudstones and marls with variable carbonate (10-35 wt%) and fossil content. Silt-sand grains are subangular quartz, rare feldspar (mostly microcline, rare albite), and shell debris; micas are biotite and muscovite. In addition, rounded phosphate and glauconite grains are present, though generally below a few percent. The marl is burrowed and the diffusive, burrow-mottled background fabrics are overprinted by discrete traces including *Planolites*, *Thalassinoides*, and *Chondrites*. Fossils that could be determined in the core include mollusks and mollusk fragments, for instance, nuculanids (e.g., *Nuculana corbicula*) and oysters. Gastropod shells, including *Acmaea* and the high-spirred *Haustator bilira*, as well as scaphopods (e.g., *Denta-*

TABLE 1 | **Detection limits (Det. I) and correlation coefficients (Corr. Ti) for major and trace elements with the Ti contents.**

	Fe_2O_3	MnO	CaO	K_2O	Cu	Zn	As	Rb	Sr	Y	Zr	Ba	La	Ce	Pb
	wt%	ppm	wt%	wt%	ppm	ppm	ppm	ppm	ppm	ppm	ppm	ppm	ppm	ppm	ppm
Det. I	–	5	–	–	5	4	5	10	1	3	5	5	10	10	5
Corr. Ti	0.64	0.44	-0.88	0.71	0.38	0.62	-0.07	0.89	0.09	0.71	0.75	0.91	0.56	0.73	0.89

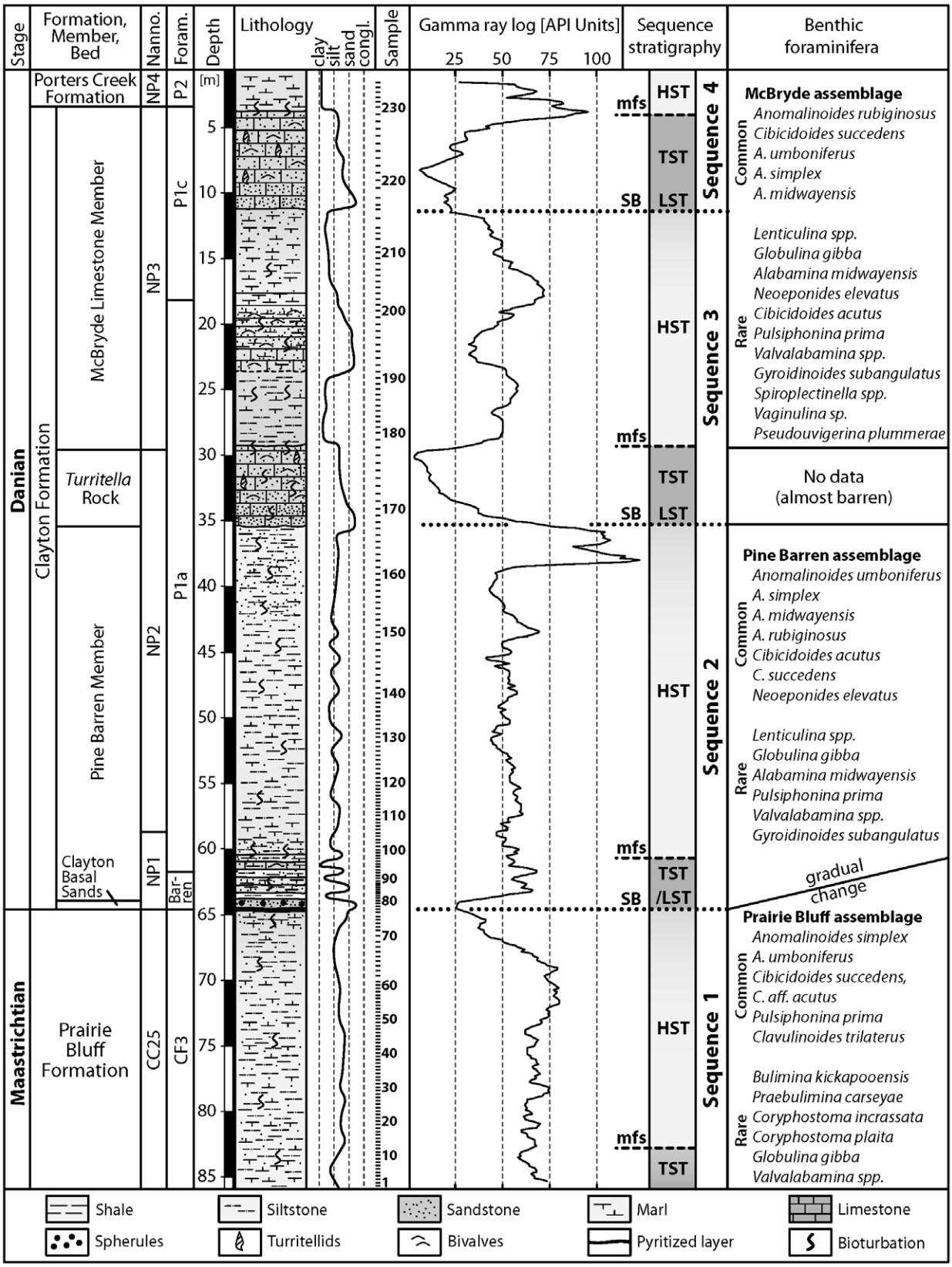

FIGURE 2 | **Stratigraphy, lithology, grain size, and gamma ray log of the Antioch Church core in combination with the composition of benthic foraminifera assemblages. Three assemblages can be recognized: the Prairie Bluff assemblage, the Pine Barren assemblage, and the McBryde assemblage (including basal Porters Creek). The latter two are typical Midway assemblages and differ mainly in relative proportions of the taxa. The Prairie Bluff and Pine Barren assemblages differ significantly in composition.**

lium), fish vertebrae, ostracods, and benthic foraminifera are also present. In the interval from 70 to 66 m in core depth, the Prairie-Bluff becomes sandy-silty mudstone with reduced fossil and carbonate content; planktic foraminifera are very rare (Figs. 2, 3). Increasing silt and clay contents are also revealed by the fore-stepping gamma log motif (Fig. 2). In contrast, the uppermost two meters of the Prairie Bluff formation are rich in carbonate (Fig. 3) and bear more abundant fossils including bivalve shell fragments, benthic foraminifera, and slightly more common planktic foraminifera.

Clayton Formation

Clayton Basal Sands

The 90 cm thick Clayton Basal Sands start with a single, 5-cm thick core piece of sandstone with a pyritized matrix (Fig. 3). This sandstone is very rich in quartz (>75%) and almost devoid of carbonate (<2%). The overlying coarse-grained white quartz sandstone is calcite-cemented (Figs. 3, 4A, B). Sedimentary structures include normal grading with very coarse sand at the base to mean sand at the top. The topmost part also shows faint lamination. Bioturbation was not observed throughout this interval. The middle part of this sand bed shows high porosity. The petrographic composition of the Clayton Basal Sands reveals more than 50% angular quartz and feldspar, including microcline, orthoclase with tourmaline inclusions, and myrmekite (quartz-feldspar intergrowths that are commonly found in plutonic rocks, see Fig. 4A). In addition, glauconite, muscovite, illmenite, as well as rare glauconized and pyritized planktic and benthic foraminifera are present. Occasionally, charcoal and leaf tissue was found. The accessory minerals myrmekite and epidote suggest an igneous and/or metamorphic protolith (García et al., 1996).

A prominent component of the lower 20 cm of the Clayton Basal Sands is mm-sized vesicular brown-green 'spherules' (Fig. 4B). Some spherules are composed entirely of calcite with a thin opaque coating and remains of bubbly inclusions lined by opaque minerals. Spherules are morphologically similar (size, shape, internal textures etc.) to Chicxulub ejecta spherules found in the Clayton Basal Sands of other KP outcrops in Alabama (Smit et al., 1996), as well as in K-P outcrops in Texas (Schulte et al., 2006), in Mexico (Schulte and Kontny, 2005), and in the Western Interior (Bohor and Glass, 1995).

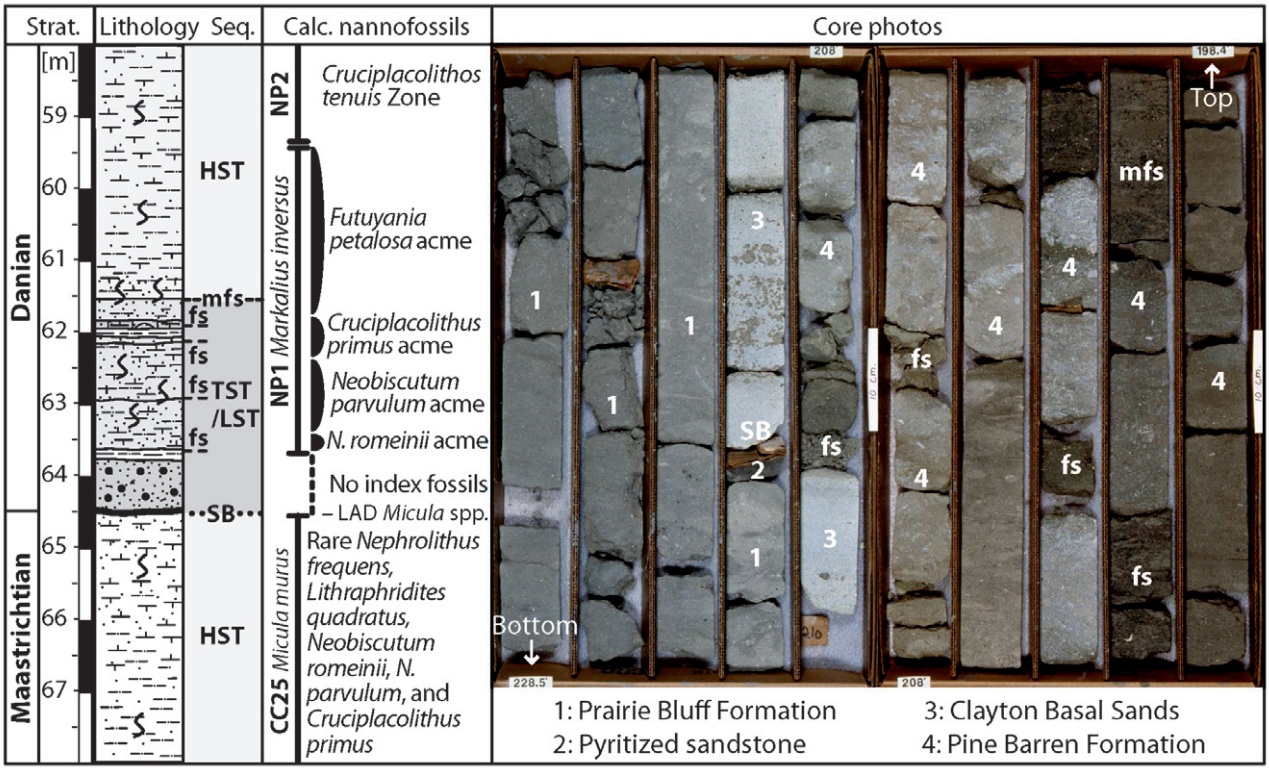

FIGURE 3 | **Lithology and core photos of the K-P transition in the Antioch Church core along with sequence stratigraphic interpretation and calcareous nannofossil biostratigraphy (Strat., stratigraphy; Seq., sequence stratigraphy). Note white Clayton Basal Sands in the core photo overlain by several prominent dark-colored flooding surfaces (Legend in Figure 2).**

Pine Barren Member

Above the Clayton Basal Sands, the lower part of the Pine Barren Member of the Clayton Fm reveals a stacked set of cm-thick glauconitic mudstone intervals, each associated with a minor GR-peak, alternating with dm-thick sandy and bioclast-rich marls (Figs. 3, 4C). About four meters above the base of the Clayton Sands, strata consist of 50-75% glauconite grains (Figs. 3, 4D). The glauconite replaces pellets, foraminifera, bookmark mica, and bryozoans, or consists of rounded grains without an internal structure. The bright green colors and the rareness of cracks ("critter manure") both suggest a juvenile, less evolved state of the glauconite (Amorosi, 1995), as also revealed by 4-6 wt% K_2O contents from electron microprobe data. The glauconite-rich interval furnishes bivalves, including *Venericardia*, and *Chlamys*, in addition to mollusk shell debris and benthic as well as planktic foraminifera; it is strongly bioturbated by *Thalassinoides* and *Chondrites*. Above the glauconite layer, the degree of bioturbation is reduced and constituents show well-developed palisade cement (Fig. 4E). Further upsection, dm-thick mudstone-marl-limestone couplets suggest cyclic variations in detritus input versus carbonate productivity (Figs. 2, 5). The uppermost part of the Pine Barren Member (40 to 35 m in core depth) is of dark color, very silty, nearly devoid of macrofossils, and associated with a pronounced GR peak.

Turritella Rock

Six meters of well-indurated, white-yellow sandy bioclastic limestone disconformably overlie the dark mudstones of the Pine Barren Member (Fig. 2). Due to the abundance of the gastropod *Turritella*, particularly, *T. mortoni*, this sandy limestone bed is referred to informally as *Turritella* Rock. The basal two meters are coarse calcareous quartz sandstone with feldspars and mica as well as abundant glauconite. In the uppermost 4 m of the *Turritella* Rock, there is an abrupt increase in fossil and matrix content, concomitant to a decrease in quartz, compared to the interval below (Fig. 4F). Pyritized and glauconized particles are prominent constituents of this sandy limestone, as well as large (up to cm-sized) aggregate grains; some ooids have also been observed. Porosity is high and in the range of 20 to 25%. Notably, iron coatings that are commonly associated with dissolution features line most of the cavities; spar cement is rarely present in this limestone. Further prominent diagenetic features include 'steinkerns' with internal sediment (micrite, quartz grains). Dissolution may have selectively affected certain bioclasts including aragonitic turritellids, but may have also been pervasive, and formed caverns of various sizes. The fauna is dominated by molds of *Turritella* shells. Additional fossils in this limestone include bivalve fragments (e.g., *Venericardia*, oysters), abundant benthic (mainly rotaliidae and miliolidae), and rare planktic foraminifera, bryozoan fragments, echinoderm spines, sponge spicules, dasycladaceans, and ostracods. The topmost 25 cm of the *Turritella* Rock are indurated, enriched in glauconite and phosphate, and bioturbated, indicating a pervasive hardground formation. The presence of irregular "foamy" calcified structures (Fig. 4G), interpreted as *Microcodium* (Alonso Zarza et al., 1999), along with the presence of meniscus-shaped as well as dripstone cement (Fig. 4H) suggests temporal emersion of the *Turritella* Rock above sea level in line with incipient soil formation (Tucker and Wright, 1992).

McBryde Limestone Member

Alternating sets of marls, siltstones, and sandy limestones of the McBryde Limestone Member of the Clayton Fm disconformably overlay the *Turritella* Rock (Fig. 2). Their character changes from dark grey, fossil-free, clayey siltstones to light grey, slightly shelly chalky marls and light grey, sandy limestones. Phosphate and glauconite are very rare in these units and only abundant at the hardgrounds atop of the sandy limestone beds at 20 m and 4 m in core depth. No evidence, however, was found for emersion above sea level at these limestone beds. The sandy limestones may be classified as bioclastic packstone, though they show significant lower grain size of the detrital and bioclastic components than, for instance the *Turritella* Rock. They bear many bivalve shells and shell fragments (e.g., *Venericardia wilcoxensis*, oysters), whereas gastropods (e.g., turritellids) are rare. The nautiloid *Hercoglossa ulrichi* was found at 21.9 m in core depth; hence, this particular limestone bed was identified as the informal '*Hercoglossa* limestone'. The marl beds usually have a mottled appearance, are bioturbated by *Chondrites* and *Thalassinoides*, and contain only few macrofossil shells or shell debris, but are relatively rich in planktic foraminifera.

Porters Creek Formation

The topmost 4 m of the Antioch Church core belong to the upper Danian 'lower' Porters Creek Fm and consist of light grey, sandy-silty marls that disconformably overlay the McBryde Limestone Member.

BIOSTRATIGRAPHY

The biostratigraphy of the Antioch Church core is based on calcareous nannofossil and planktic foraminiferal records. Calcareous nannofossils reveal an impoverished and poorly to modestly preserved upper Maastrichtian assemblage and more diverse and commonly better pre-

served Danian assemblages. Following the biozonation schemes provided by Martini (1971) and Perch-Nielsen (1985), a succession of five calcareous nannofossil zones have been distinguished for the late Maastrichtian to Danian (Fig. 2): The *Micula murus* Zone (CC25, upper Maastrichtian), the *Markalius inversus* Zone (NP1, lowermost Danian), the *Cruciplacolithus tenuis* Zone (NP2, lower Danian), the *Chiasmolithus danicus* Zone (NP3, middle Danian), and the *Ellipsolithus macellus* Zone (NP4, upper Danian).

Danian planktic foraminiferal biostratigraphy is somewhat hampered because planktic foraminifera are very rare to absent throughout the core. In addition, diagnostic taxa such *Subbotina triloculinoides* may be almost absent because of ecological exclusion in shallow waters. Under these circumstances, it is unlikely that all commonly used Danian zonal markers are present from the onset of their ranges upwards. Consequently the foraminiferal zonation must be considered only tentatively. The upper part of the Prairie Bluff Fm contains the marker species *Gansserina gansseri*, which indicates Maastrichtian Biozone CF3 (Pardo et al., 1996). The two upper Maastrichtian biozones CF1 and CF2 are missing in this section. Washed residues from the lowermost three meters above the base of the Clayton Basal Sands provided no planktic foraminifera. At ~62 m in the lower Pine Barren Member, rare but well preserved specimens of *Eoglobigerina edita*, *Praemurica taurica*, and *Globoconusa daubjergensis* were observed. These taxa range from Zone Pα to P1c (Olsson et al., 1999). Their minute size (<100 μm) and absence of larger taxa suggests that this level may be representing the lower range of these taxa. However, *Parvularugoglobigerina eugubina*, the zonal marker of Pα was not observed, and consequently subzone P1a is the appropriate biostratigraphic allocation. Higher up in subzone P1a (upper Pine Barren Member and lower McBryde Limestone Member), *Praemurica pseudoinconstans* is the most common species (>125 μm) in samples that are somewhat richer in planktic foraminifera. The lowest occurrence of *Subbotina triloculinoides* (one specimen) coincides with the lowest representatives of *Praemurica inconstans* at 17 m in core depth, marking the base of Subzone P1c. Since the FAD of *Subbotina triloculinoides* marks the base of Subzone P1b, this suggests that Subzone P1b is entirely missing. Considering that *S. triloculinoides* is a deeper thermocline dweller amongst planktic foraminifera (Berggren and Norris, 1997), it is likely that the shallow depths cause its rarity during deposition of the Pine Barren Member. Consequently, the absence of subzone P1b is rather ecologically controlled than the result of a large hiatus at ~20 m. The Porters Creek Fm yields rare taxa, such as *Globanomalina ehrenbergi* and *Praemurica uncinata* indicating Zone P2 (Berggren et al., 1995; Olsson et al., 1999) at the top of the core.

Remarkably, biostratigraphic boundaries frequently coincide with sequence boundaries or flooding surfaces (e.g., top of the Prairie Bluff Fm, the top of the *Turritella* Rock and the top of the McBryde Limestone Member) at which a hiatus of unknown duration due to erosion exists. For instance, the presence of well-preserved *Gansserina gansseri* in the topmost centimeters of the Prairie Bluff as well as the absence of *Micula prinsii* suggest that the uppermost Maastrichtian (Zone CC26) is not preserved in the Antioch Church core and a hiatus of at least 0.6 My exists atop of the Prairie Bluff. In addition, the absence of a distinct *Thoracosphaera* acme at the base of Biozone NP1, which is generally observed directly above the K-P boundary clay (Gardin, 2002), suggest a hiatus and/or erosion atop of the Clayton Basal Sands, as also observed by Moshkovitz and Habib (1993) for the Braggs and Mussel Creek sections. However, for the remaining lower Danian Biozone NP1 (see Fig. 3), the presence of successive acmes of *Neobiscutum romeinii*, *Neobiscutum parvulum*, *Cruciplacolithus primus*, and *Futyania petalosa* during the lowermost Danian suggests a stratigraphically complete succession. In addition, *Prinsius dimorphosus* is present in the uppermost samples of this interval. An analogous succession has been found to occur within Biozone NP1 in several other K-P boundary sections worldwide, including El Kef, Tunisia, and Brazos, Texas (Gartner, 1996; Gardin, 2002; Schulte et al., 2006).

BENTHIC FORAMINIFERAL ASSEMBLAGES

Recently, K-P benthic foraminiferal assemblages from Alabama were studied by Olsson et al. (1996) from two cores at Millers Ferry, located some 80 km WNW of Antioch Church (Fig. 1). The benthic foraminiferal distribution patterns were interpreted in terms of variations of substrate and paleodepth, the latter based – in part – on

FIGURE 4 | **A) Clayton Basal Sands with a large feldspar fragment. B) Detail of an ejecta spherule with globular inclusions. C) Sandy limestone above Clayton Basal Sands with glauconite and foraminifera, as well as shell and bryozoan fragments. D) Maximum flooding surface with abundant glauconite. Most glauconite is probably derived from fecal pellets. Note bright green color of glauconite, which is indicative of a nascent evolutionary state, involving a short time of formation (<50 ka; Amorosi, 1995). E) Glauconite grains with bladed marine cements from the upper condensed section overlying the maximum flooding surface. F) *Turritella* Rock with quartz, phosphate, bioclastic debris and ghosts of diagenetically dissolved gastropod shells. G) Steinkern of a gastropod shells with micrite infilling. The upper part of the gastropod is eroded and replaced by an irregular cellular structure interpreted as *Microcodium*. This structure is commonly an indicator for incipient stages of soil formation and hence suggests temporarily subaerial exposure of the *Turritella* Rock. H) Dripstone cement below a mollusk shell in the *Turritella* Rock.**

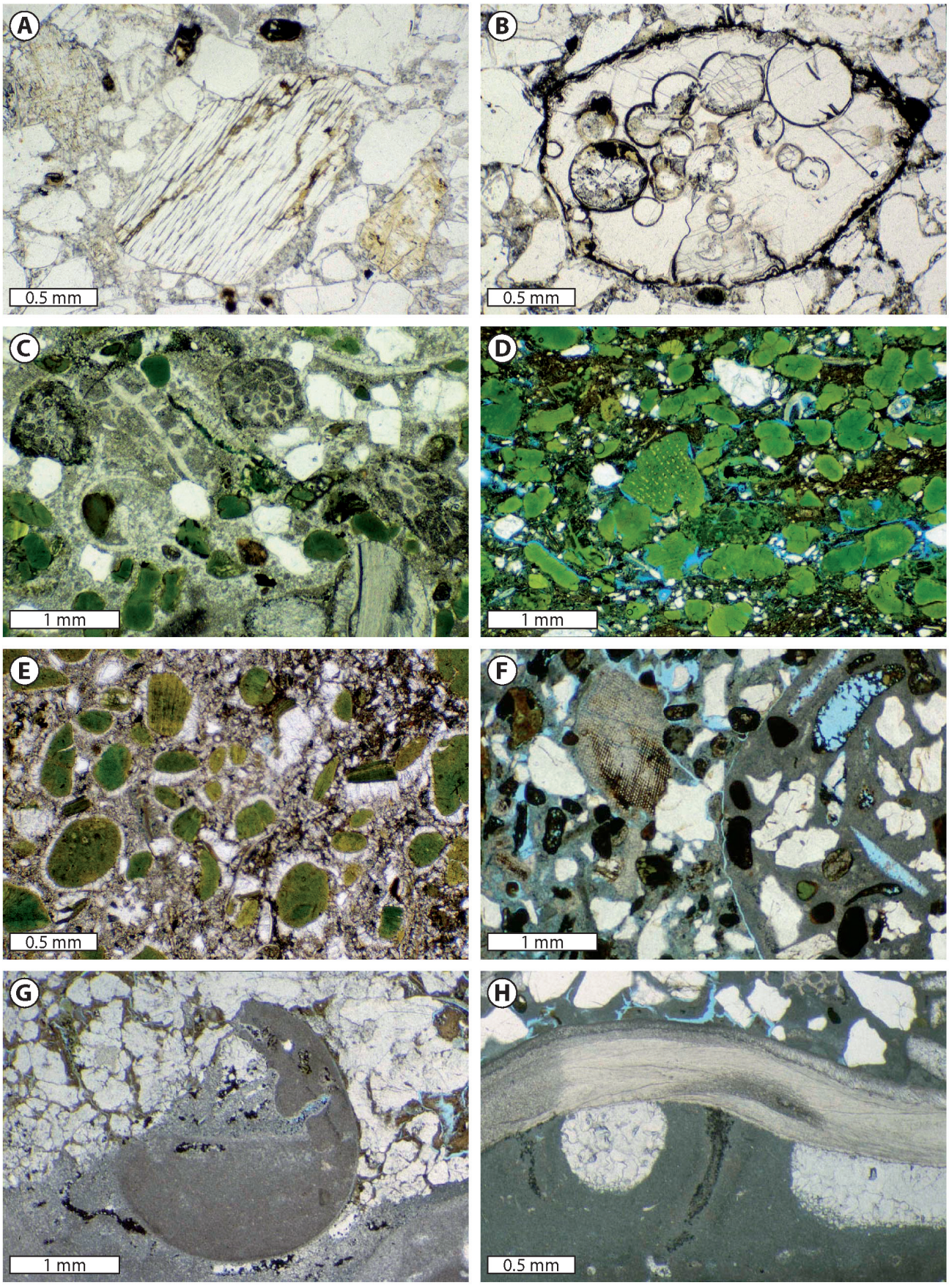
A
0.5 mm
B
0.5 mm
C
1 mm
D
1 mm
E
0.5 mm
F
1 mm
G
1 mm
H
0.5 mm

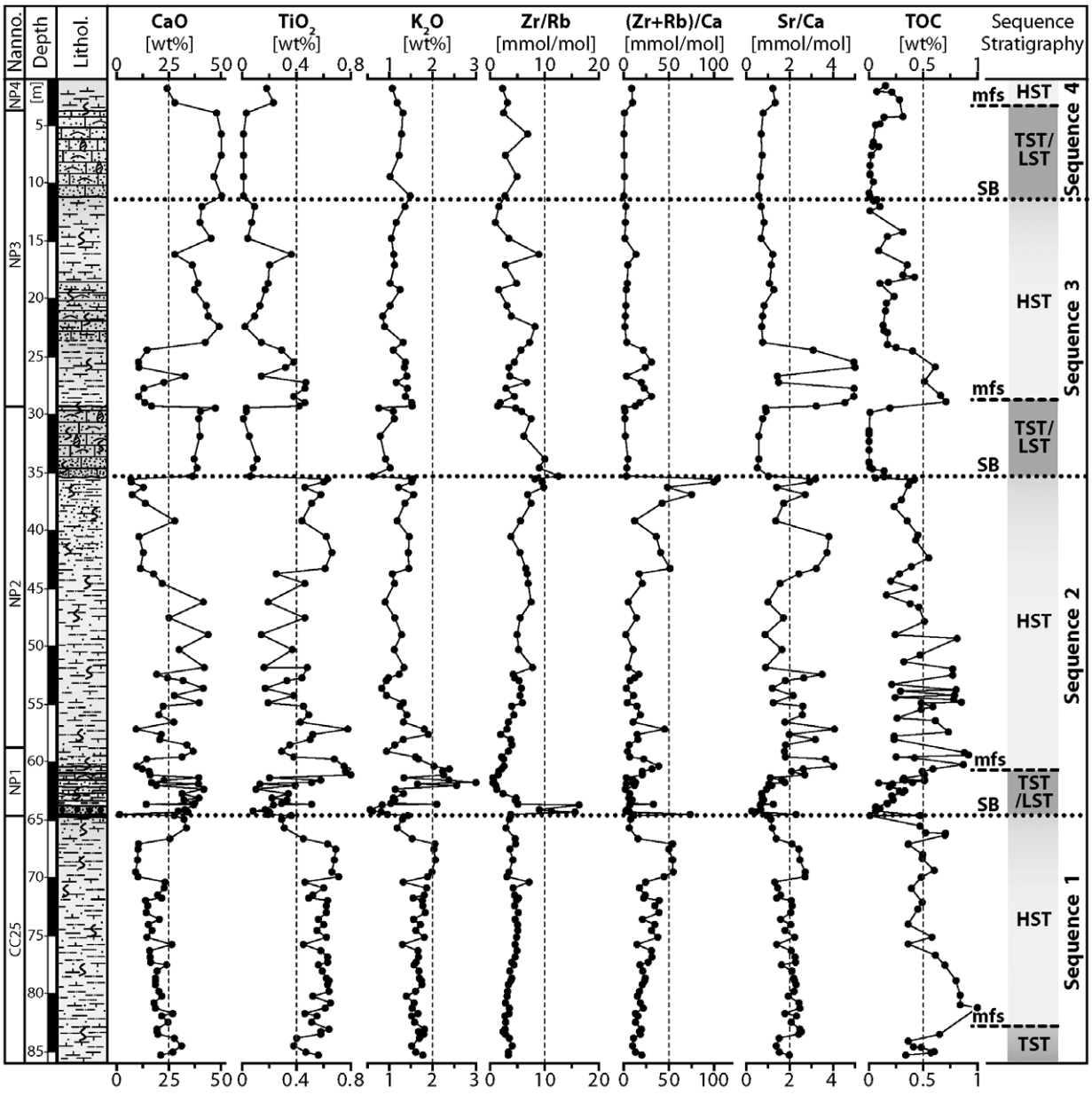

FIGURE 5 | **Selected major and trace elements and element ratios from the energy-dispersive X-ray fluorescence spectrometry of the Antioch Church core. In addition, the total organic content (TOC) is shown. Further element geochemical data are shown in Table A1 (online at www.geologica-acta.com).**

the paleoslope models of New Jersey (Olsson and Nyong, 1984). A quantitative benthic faunal analysis based on the fraction >63 μm revealed a sequence of assemblages indicating paleodepth ranging between 30 and 100 m. In the following and in Fig. 2, we provide an overview of the composition of the foraminiferal assemblages (size fraction >125 μm) and of assemblage changes from the upper Cretaceous into the lower Paleocene.

The topmost 20 m of the upper Maastrichtian Prairie Bluff Fm in the Antioch Church core contains a low diversity benthic assemblage with common to abundant *Anomalinoides simplex*, *A. umboniferus*, *Cibicidoides succedens*, *C. aff. acutus*, *Pulsiphonina prima*, *Clavulinoides trilaterus*, and subordinate *Bulimina kickapooensis*, *Coryphostoma incrassata*, *C. plaita*, *Globulina gibba*, *Valvalabamina spp.*, *Lenticulina spp.*, *Dorothia bulletta*, and *Spiroplectinella sp*. Planktic foraminifera are quite rare, composing up to 5%. The assemblage of the uppermost 2 m of the Prairie Bluff is similar, but slightly more diverse. Particularly endobenthic morphotypes such as *C. incrassata*, *C. plaita* and *Praebulimina carseyae* are much more common. This interval also contains more planktic specimens (5-10%).

The lowermost Paleocene assemblage of the Clayton Basal Sands bears resemblance to the upper Maastrichtian assemblage, but also includes new taxa, notably *Alabamina midwayensis*, *Cibicidoides acutus*, *Neoeponides elevatus*, and *Anomalinoides rubiginosus*. These taxa are characteristic Paleocene so-called Midway-type taxa that are known to have occurred worldwide (Berggren and Aubert, 1975). At the same time other taxa, typical for Maastrichtian deposits worldwide have their highest occurrences within or below the Clayton Basal Sands: *C. plaita*, *C. incrassata*, *P. carseyae* and *C. aff. acutus*. These sands also yield 1-2% planktic taxa, including large specimens of *Rugoglobigerina* and *Heterohelix*, besides smaller *Guembelitria*. Since the larger planktic taxa did not survive into the Danian (Olsson and Liu, 1993), these specimens are considered reworked from Maastrichtian deposits. The lower part of the Pine Barren Member does neither contain Cretaceous planktic taxa (>125 μm), nor the abovementioned typical Maastrichtian benthic taxa. Consequently, it should be considered that the Maastrichtian benthic taxa of the Clayton Basal Sands are in part likely to have been reworked.

Further upsection, the Pine Barren Member up to the base of the *Turritella* Rock, yields low-diversity assemblages with common to abundant *Anomalinoides* – including *A. umboniferus*, *A. simplex*, *A. midwayensis*, and *A. danica* – as well as *C. acutus*, *C. succedens* and *N. elevatus*. Accessory taxa are *Lenticulina spp.*, *Globulina gibba*, *P. prima*, *Valvalabamina spp.* and *Gyroidinoides subangulatus*. Bi- and triserial endobenthic morphotypes are extremely rare in the studied size fraction of this interval. In addition, planktic specimens are nearly absent. A similar assemblage is present in the basal sample of the *Turritella* Rock, but the dominance of *N. elevatus*, *A. umboniferus*, *A. midwayensis* and *A. danica* is even greater than in the underlying marls and mudstones.

Assemblages of the McBryde Limestone Member and the basal part of the Porters Creek Fm are slightly more diverse than those of the Pine Barren Member, but still strongly dominated by *Anomalinoides spp.* and *Cibicidoides succedens*. The accessory faunal components of the Pine Barren Member are more common in these units and joined by *Spiroplectinella spp.*, *Alabamina midwayensis*, and *Vaginulina sp.* These units also contain more numerous planktic taxa (3-10%). A sample from the uppermost limestone bed of the McBryde Limestone Member is very similar to those of the surrounding beds, but it contains <1% planktic foraminifera. This low number may be a primary signal, but the preservation of the assemblage is relatively poor compared to those from the more clayey units and taphonomic reduction of the relative abundance of planktic foraminifera cannot be excluded.

MAJOR AND TRACE ELEMENT GEOCHEMISTRY

The results from main and trace element analyses by energy-dispersive X-ray fluorescence spectrometry (EDS) of samples from the entire Antioch Church core are shown in Fig. 5 (the original data is provided in Table A1, available online at www.geologica-acta.com). In addition, the Zr/Ti and Sr/Ca ratio is shown in Fig. 5 to depict changes in the terrigeneous and carbonate phases, respectively. Several elements (Cu, As, Nb, La, Y), however, showed a close correlation to the Ti contents and have been omitted in the graphs for brevity reasons; yet, their correlation coefficient to the Ti contents and their individual concentrations are presented in Table 1.

To characterize the immediate K-P transition, additional wavelength-dispersive X-ray fluorescence spectrometry (WDS) analyzes of closely spaced samples from the interval 58 to 68 m across the K-P boundary were conducted and selected elements, including Si, Ti, Fe, Mg, and K, have been normalized to aluminum and, together with the Zr/Ti and Sr/Ca ratios are depicted in Fig. 6 (original values in Table A2, available online at www.geologica-acta.com). The normalization of these elements against Al allows for enhanced monitoring of changes in the detrital composition, since these elements are generally not bound to a carbonate phase.

In general, element abundances of the Maastrichtian-Danian strata in the Antioch Church core show two opposing distribution patterns that correspond well to the key 'end member' lithologies (Fig. 5 and Table A1, available at www.geologica-acta.com): Silty-sandy mudstone and sandy bioclastic limestone, with intermediate distribution patterns constituted by silty-sandy marl. The silty mudstone intervals are characterized by low CaO content (<15 wt%) and peak abundances of elements commonly incorporated in siliciclastic detritus, including TiO_2, Fe_2O_3, K_2O, Rb, Zr, and Ba. The marls and limestones show higher values of CaO up to >50 wt%. The high negative correlation coefficients between CaO and elements commonly bound to the terrigeneous fraction (see Table 1) suggests progressive dilution of the terrigenous fraction by carbonate during intervals of elevated biogenic productivity. Only Strontium (Sr) shows no significant correlation either with CaO or with TiO_2, and therefore Sr appears to be incorporated in both fractions (presumably in feldspars as well as in carbonate).

Following the scheme developed by Dypvik and Harris (2001), we use Zirconium (Zr) and Rubidium (Rb) to

characterize the siliciclastic fraction (Fig. 5). Zr is enriched in heavy minerals and commonly associated with the relatively coarse-grained silt-sand-sized siliciclastic fraction. In contrast, Rb is commonly incorporated in micas and clay minerals and average claystones are normally enriched in Rb compared to sand or limestones. Consequently, the Rb contents may be used as a measure for the abundance of the less-than silt-sized fraction. The Zr/Rb ratio may therefore give evidence of the ratio of coarse- vs. fine-grained detritus in the sediment when comparing sediments having the same provenance. Since, as in the case of the Antioch Church core, Sr is apparently associated with both, the carbonate and the siliciclastic fraction, we modified the scheme of Dypvik and Harris (2001) by using the Ca contents to normalize the Zr+Rb contents and to get an overview on the carbonate vs. siliciclastics ratio.

A steady increase is recognized in the terrigeneous fraction during the Prairie Bluff Fm (85.5-67 m): CaO decreases during this interval from 30 to about 10 wt%, whereas all other element concentrations, except Sr, generally increase. In the interval 65 to 70 m in core depth, high ratios of the (Zr+Rb)/Ca >50 and Sr/Ca >3 are observed. In the uppermost part of the Prairie Bluff formation, the CaO content abruptly increases up to peak values of 35 wt%, while elements linked with terrigeneous detritus decrease. This trend is punctuated by the pyritized sandstone piece that has been found above the Prairie Bluff and below the Clayton Sands. This pyritized sandstone has extraordinary high abundances of Fe_2O_3 (>30 wt%), Cu (40 ppm), and As (300 ppm), whereas TiO_2, MnO, Sr, Zr, Zn, and Ba are significant lower than in the enclosing lithologies, and CaO is close to zero (<2 wt%).

The Clayton Basal Sands are characterized by very high SiO_2 contents, high Zr/Rb ratios and a CaO contents exceeding 30wt% as well as low amounts of all other major and trace elements, compared to the enclosing shales and limestones. During the lower part of the Pine Barren Member above the Clayton Basal Sands, element abundances switch immediately back to values comparable to the latest Maastrichtian Prairie Bluff Fm. At about 62 m, the drastic increase in glauconite is reflected by abundance of Fe_2O_3 (up to 15 wt%), K_2O (up to 4.5

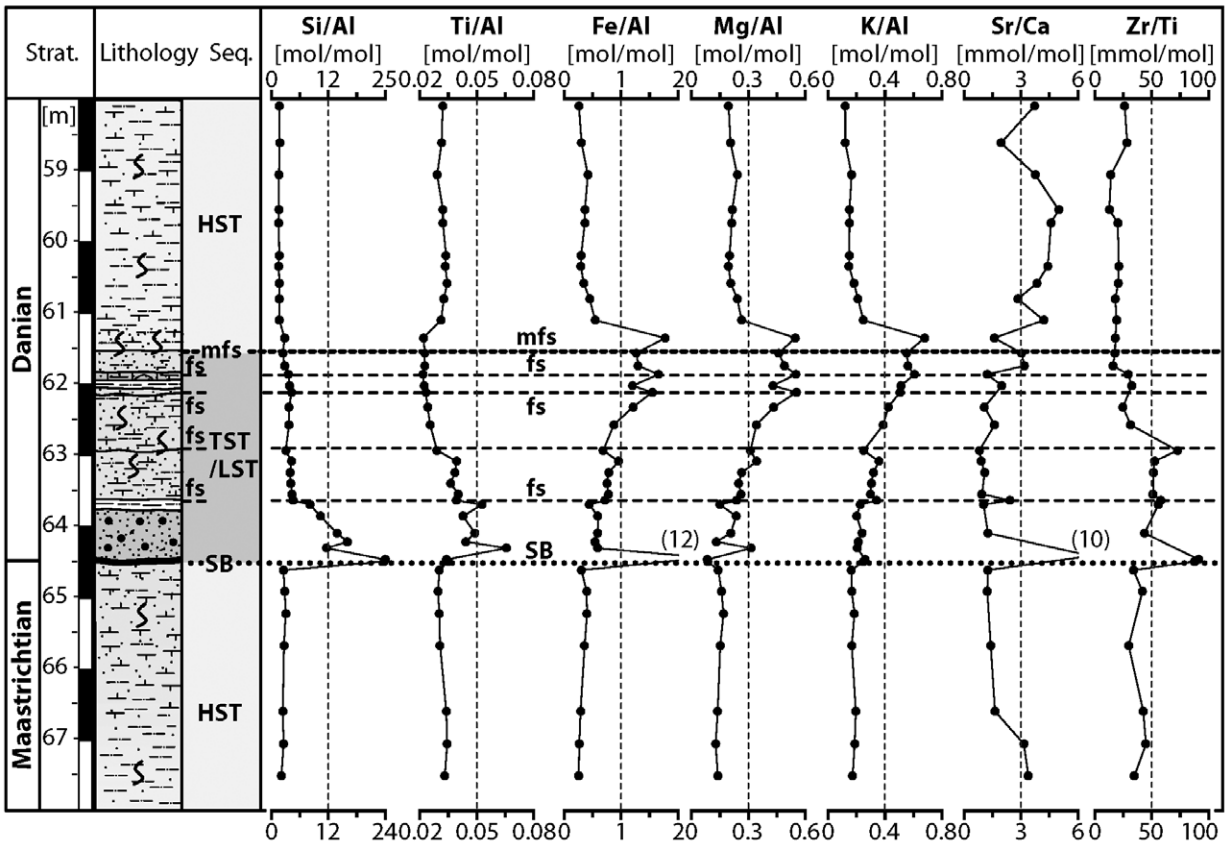

FIGURE 6 | **Selected major and trace element ratios from the wavelength-dispersive X-ray fluorescence spectrometry of the K-P transition in the Antioch Church core.**

wt%), and Rb (120 ppm). Immediately above the glauconitic maximum flooding interval, reduced carbonate values, and increased terrigeneous input followed by strong (cyclic) fluctuations in the carbonate/detritus ratio occurs. Notably, the Sr contents and the Sr/Ca (>4) ratios both show peak values. In the uppermost part of the Pine Barren Member, sediments have low carbonate contents (<10 wt%) and high values of detrital elements, including TiO_2 (>0.8 wt%) and Zr (~500 ppm), indicate mainly terrigeneous input as also shown by the exceptionally high (Zr+Rb)/Ca ratios >100.

The *Turritella* Rock is almost devoid of elements assigned to terrigeneous-derived minerals (except for quartz, as revealed by thin-section analysis), and hence, is almost 'pure' sandy limestone. The hardground atop of this limestone package has elevated Fe, Cu, As, and Zn concentrations, indicative of condensed sedimentation, as well as temporary anoxic conditions during the flooding event recognized in the overlaying shales. The overlying highstand deposits reveal increased terrigeneous input and, for instance, Sr values are significantly elevated and reach peak values above 1,000 ppm.

The McBryde Limestone Member of the Clayton Fm and the Porters Creek Fm are characterized by low fluctuations in the element abundances and a constant high carbonate content; only the marls of the Porters Creek Fm show a significant increase in elements characteristic of terrigeneous detritus.

TOTAL ORGANIC CARBON

The average organic carbon content of the sediments of the Antioch Church core is generally low and comprises about 0.5 wt% TOC for the siliciclastic-dominated Maastrichtian to lower Danian samples (Fig. 5). In contrast, during the middle Danian, carbonate-dominated part, the average is less than 0.2 wt% TOC except for the lower McBryde Limestone Member, which yields TOC up to 0.7 wt%). All samples have a very low hydrogen index (between 10 and 50 mg HC/g org. C) and an intermediate oxygen index (between 80 and 160 mg CO_2/g organic carbon), suggesting a predominance of immature terrestrial organic matter (Langford and Blanc-Valleron, 1990).

CLAY MINERALOGY

Clay minerals identified in the <2 μm fraction of the Antioch Church core and used for semi-quantitative analysis include smectite, chlorite, mica, and kaolinite. Smectite and kaolinite are the predominant clay minerals, whereas illite and chlorite are present in minor quantities. In addition, some samples are characterized by abundant zeolites. Mixed-layer clay minerals, including illite-smectite and chlorite-vermiculite, occur very rarely and have therefore not been included in the semiquantitative analysis. Three intervals with distinct clay mineralogical assemblages have been identified (Fig. 7):

Assemblage 1

A kaolinite + smectite + illite dominated assemblage is present during late Maastrichtian sequence 1 up to the maximum flooding surface of sequence 2. This assemblage shows a gradual change from kaolinite predominance (~70%) with minor smectite (~15%) to smectite predominance (~80%) with only minor amounts of kaolinite (~15%). Illite averages 10% with fluctuations in the range from 4-20%, whereas chlorite is below 5%. Only the Clayton Sands show distinct smectite enrichment (>80%) with only subordinate amounts of kaolinite (~10%) and illite (~4%). In the condensed section above the Clayton Sands, mica is enriched (25-30%). The smectite in assemblage 1 shows 'full width at half maximum' (FWHM) values in the range of 0.95 to 1.2 °2Θ. In concert with the absence of distinct smectite (002) and (003) reflections in the diffractograms, this indicates at most a moderate crystallization or large crystal sizes and promotes a detrital origin for the smectite. The illite (002/001) peak intensity ratio is 0.2 to 0.4, suggesting an intermediate biotitic to muscovitic octahedral character (Petschick et al., 1996). Higher values (>0.4) of the illite (002/001) intensity ratio are present only in the Clayton Basal Sands.

Assemblage 2

A smectite + kaolinite + illite dominated assemblage with prevalence of smectite and kaolinite is present in the Antioch Church core in sequence 2 from the maximum flooding surface up to the base of the *Turritella* Rock. In this interval, smectite averages 58%, kaolinite averages 26%, and illite has mean values of 12%, whereas chlorite is well below 5%. Smectite generally shows well-defined, narrow peaks and the FWHM values increase to average values of 0.8 °2Θ indicating a slightly higher degree of crystallinity or different grain-size compositions as compared to clay mineral facies of assemblage 1. Also, the illite (002/001) peak intensity ratios are considerably higher and show values exceeding 0.4, that in combination with the average c-lattice constant of about 9.9 Å (~8.88 °2Θ) of the illite, suggest a muscovite-like 'octahedral' character (Petschick et al., 1996).

Assemblage 3

A smectite + illite dominated assemblage is present in the Antioch Church core in sequence 3 and 4 and includes smectite (~85%) largely dominating over illite (~14%), whereas kaolinite and chlorite are virtually absent (<2%). In addition, zeolites (clinoptilolite and heulandite) are constantly present. The *Turritella* Rock and the upper part of the McBryde Limestone Member as well as the Porters Creek Fm show higher smectite and lower illite contents. The smectite has well-defined, narrow peaks with FWHM values averaging 0.7 to 0.8 °2Θ. The illite (002/001) peak intensity ratios are between 0.15 and 0.4, pointing to a biotitic to muscovitic octahedral character (Petschick et al., 1996).

INTERPRETATION AND DISCUSSION

First, we will interpret the combined sedimentological, petrographical, and geochemical data of the Antioch Church core within the sequence stratigraphic setting given by previous studies for the Alabama Gulf of Mexico margin (Baum and Vail, 1988; Donovan et al., 1988; Mancini and Tew, 1993). Second, we will discuss the magnitude of facies changes and the results from the benthic foraminiferal assemblages, which allow for providing quantitative estimations of water depth changes. Third, we will outline the depositional nature of the K-P event bed, before we conclude the discussion with inferences for paleoclimate changes from the clay mineral facies.

Sequence stratigraphic setting

Sequence 1

The first sequence, or to be more accurate, upper part of a sequence, comprises the Prairie Bluff Fm that is inferred to represent a highstand systems tract (Mancini et al., 1996). In the lowermost, more calcareous part of this sequence in the Antioch Church core (3 to 86 m in core depth), a diverse marine fauna, including sparse planktic foraminifera, represents open-marine conditions. According to Mancini et al. (1996, fig. 10), this part of the Antioch Church core may be correlated to the maximum flooding surface in the Prairie Bluff Fm that is in the upper part of the *A. cymbiformis* Zone (CC25) or the lower part of the *M. murus* Zone (CC26). This maximum flooding surface and overlying highstand depositional systems tract of the Prairie Bluff Fm are recognized throughout central Alabama and eastern Mississippi (Mancini et al., 1996).

In the upper part of sequence 1 (69-73 m in core depth), the sandy shales and marls of the Prairie Bluff show a marked increase in the amounts of elements bound to terrigeneous minerals including TiO_2, K_2O, Rb, Zr, and Ba, as well as a decrease in carbonate. An increasingly shaley (or condensed) character is also revealed by increasing gamma-ray counts in the upper part of this sequence around 70 m in core depth (Fig. 2). The increase in siliciclastic detritus is coupled with reduced diversity in marine fossils and almost absence of planktic

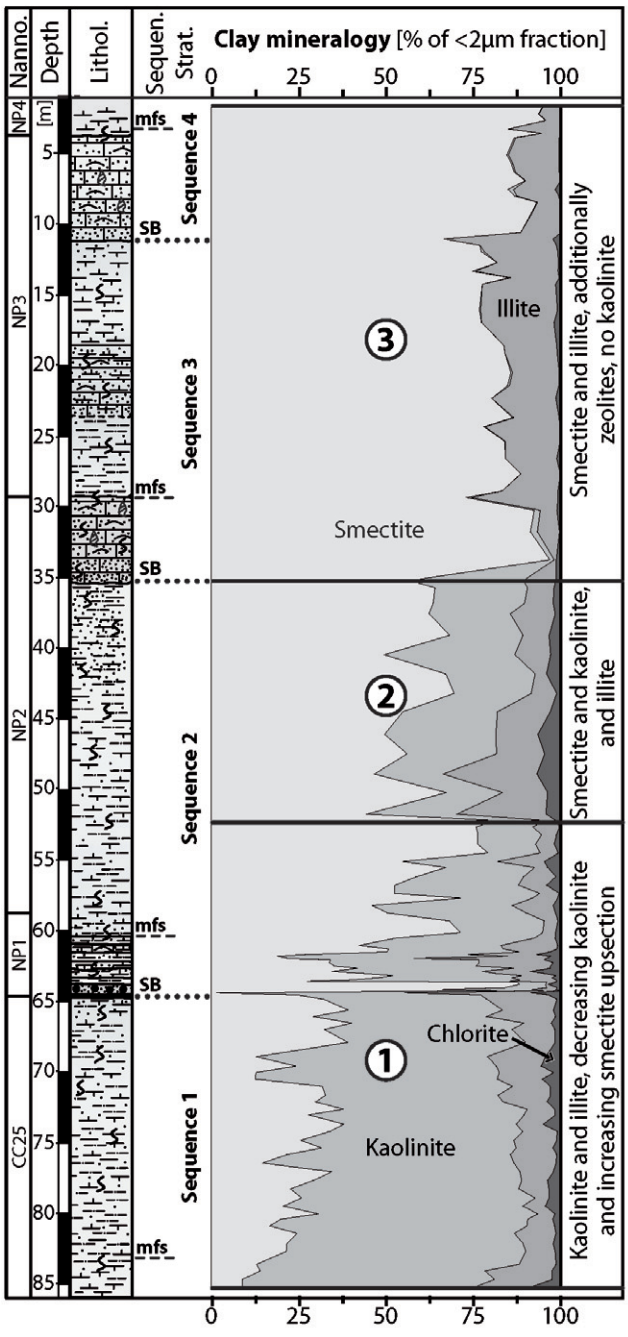

FIGURE 7 | **Clay mineralogy of the Antioch Church core. Data is given as relative percent of the glycolated <2 µm fraction with correction factors (Biscaye, 1965).**

foraminifera. Therefore, this interval, which is also marked by high Sr/Ca and (Zr+Rb)/Ca ratios, may be interpreted as a progradational facies development. However, in the uppermost part of the Prairie Bluff Fm at Antioch Church (65 to 68 m in core depth), the carbonate content rises from 15 to 30 wt% – and in concert with the slightly more common presence of planktic foraminifera – may suggest deepening of the depositional environment.

Sequence 2

The second sequence comprises the Pine Barren Member of the Clayton Fm. Its lower surface is marked by the Clayton Basal Sands that are characterized by a pronounced back-stepping gamma log motif and an increase in grain-size of terrigeneous detritus (Fig. 2). Since the Clayton Basal Sands include rare planktic foraminifera and calcareous nannofossils indicative of open-marine conditions (see also Olsson and Liu, 1993), this may suggest that sea level did not fall beyond the shelf break, though previous studies have concluded otherwise (Baum and Vail, 1988; Donovan et al., 1988). Therefore, this sequence boundary is classified as type-2 sequence boundary *sensu* Van Wagoner et al. (1990), since no evidence for subaerial exposure or fluviatile influx was observed. This interpretation is in line with previous studies (Donovan et al., 1988) that placed the sequence boundary atop of the Prairie Bluff Fm to coincide with the base of the Clayton Fm since the Clayton Basal Sands have long been considered as bar sands or incised valley fill deposits genetically linked to a sea-level lowstand (Baum and Vail, 1988; Donovan et al., 1988; Mancini and Tew, 1993). However, alternatively, the Clayton Basal Sands have been interpreted as tsunami deposit associated with the Chicxulub impact (Olsson et al., 1996; Smit et al., 1996).

Above the Clayton Basal Sands, the lower part of the Pine Barren Member reveals a stacked set of thin fine-grained shale intervals enclosing dm-thick sandy and bioclast-rich marls. The mica-rich shale layers are interpreted as flooding surfaces (Van Wagoner et al., 1990) and the 'shale-marl couplets' may be considered as parasequences that record slight variations in sediment input, distal-proximal setting, and/or relative sea level within an overall transgressive setting. The transgressive trend is terminated at the glauconitic maximum flooding surface about four meters above the base of the Clayton Basal Sands (Fig. 2). A similar position of the maximum flooding surface during the upper part of the *M. inversus Zone* (NP1) has been observed in sections throughout Alabama (Baum and Vail, 1988; Donovan et al., 1988; Van Wagoner et al., 1990). The switch to increased siliciclastic sedimentation – that takes place about 2 m above the glauconite interval maximum flooding surface – is interpreted to mark the beginning of the prograding highstand systems tract of sequence 2. However, throughout the lower part of the highstand, between 45 and 55 m in core depth, dm-thick mudstone-marl-limestone couplets suggest variations in detritus input versus carbonate productivity and are interpreted as parasequences (Figs. 2, 4, 5).

In the uppermost, very silty part of the highstand systems tract of sequence 2 immediate below the *Turritella* Rock, trends include reduced carbonate content, as low as <10 wt%, and progressively increasing terrigenous input associated with a pronounced GR peak as well as very high Zr/Rb, (Zr+Rb)/Ca and Sr/Ca ratios. Since these deposits are not particularly enriched in mica, potassium, or organic matter, we suspect that the high gamma ray readings are due the presence of Thorium since this element occurs in sand- and silt-sized grains of certain heavy minerals (e.g., Monazite and Zircon; Rider, 1996). Elevated Th concentrations are attributed to the sorting and concentration of heavy mineral grains by waves breaking on the foreshore, and heavy mineral concentrations are a common and diagnostic feature of foreshore deposits (Hampson et al., 2005). Consequently, the uppermost silty part of the Pine Barren Member is interpreted as regressive highstand systems tract associated with a rapid seaward progradation of facies belts and suppression of biogenic carbonate formation (Van Wagoner et al., 1990).

In conclusion, sequence 2 includes a transgressive interval with low sedimentation rates during the earliest Paleocene. The transgressive part is about 4 m thick and corresponds to the lower thirds of Biozone NP1 with ≤0.5 systems tract, which corresponds to the large part of Biozone NP2, is about 25 m thick and has a duration of 0.5-0.6 My, suggesting an almost threefold increase of sedimentation rates, related to the progradational development of strata.

Sequence 3

The deposition of the *Turritella* Rock records a pronounced change in the depositional mode, hydrodynamic regime, and mineralogical composition of the sediment. The vertical sedimentary succession within this sand-limestone package corroborates a rising sea level, mainly owed to the upward increase in micrite which occurs concurrent to a decrease in quartz content (Fig. 2, 3). Therefore, the base of the *Turritella* Rock is interpreted as a type-2 sequence boundary, which is overlain by a lowstand and transgressive systems tract. There is no sharp boundary between the lowstand and transgressive systems tract since no marked flooding surface was observed within the *Turritella* Rock. Mancini and Tew (1993) have drawn an analogous conclusion, though the *Turritella* Rock was termed 'shelf margin systems tract' by these

authors. Following deposition of the *Turritella* Rock, however, water depth, decreased temporarily, resulting in emergence and influx of surface waters in the vadose zone, as indicated by the petrologic studies. This temporal emergence within an allover rising sea level trend may be related to parasequences, with short-term stops of sea-level rise and subsequent filling of the accommodation space. Since water-depth was presumably very low (within storm or even wave base (see following paragraphs), even small-scale sea level fluctuations may have led to emergence above sea-level.

The limestones of the *Turritella* Rock are overlain by a shale interval that, on a first glance, corresponds in composition and abundance of petrological and geochemical phases to the silty shales immediately below these limestones (Figs. 2, 4). However, the trace element concentrations, show significant differences: The elevated Sr (up to >1000 ppm) as well as very low Zr concentrations <30 ppm suggests variations in the provenance of these shales. The lowered fossil content in the McBryde Limestone Member, as compared to the *Turritella* Rock, as well as the significantly smaller grain-size of the components, and decreased amounts of coarse silicic detritus, suggest a more distal depositional environment. Open-marine conditions are also indicated by the presence of nautiloids, and more common planktic foraminifera in the marl intervals. The maximum flooding surface is recorded by a prominent peak in the gamma log, as well as a peak in the TOC values at about 29 m in core depth, and occurred in conjunction with increased planktic foraminiferal abundances. The overlying highstand systems tract shows two 10 m-thick marl-limestone cycles that are interpreted as parasequences.

Sequence 4

The marly limestones and marls of the top of the McBryde Limestone Member show a similar succession of lithofacies when compared to the *Turritella* Rock, suggesting a related pattern of basal sequence boundary, subsequent lowstand and transgressive systems tract, followed by a highstand systems tract (Figs. 2, 4). Nevertheless, in sequence 4, the lithofacies development suggests that environmental changes are not as pronounced as in sequence 3 below: The lowered fossil content, as compared to the *Turritella* Rock, as well as the significantly smaller grain-size of the components and the increased amounts of silicic clayey detritus, suggest less pronounced proximal-distal trends, and probably more open-marine conditions with lower energy of the hydraulic regime.

In conclusion, the succession of facies shifts associated with the various systems tracts can be well resolved by element data and various element ratios including Zr/Rb, (Zr+Rb)/Ca, and Sr/Ca. Very high Zr/Rb ratios (>10) occur around sequence boundaries whereas very low Zr/Rb ratios (<1) are found around maximum flooding surfaces. This pattern of Zr/Rb ratios may suggest increased winnowing of fine clayey particles and enrichment of residual minerals, probably indicating enhanced current activity during lowering of relative sea level and vice versa. The (Zr/Rb)/Ca ratio shows also maximum values during the late highstand – probably due to the suppression of carbonate productivity. However, peak ratios of (Zr/Rb)/Ca are also found during across maximum flooding surfaces (e.g., at 60 m in core depth), reflecting the lower carbonate productivity in deeper water, when compared to higher productivity in shallow near-shore settings during the transgressive systems tract. High Sr/Ca (>4) ratios are generally found for transgressive intervals and lower Sr/Ca ratios (<4) values are present during the late highstand.

Additional information on sea level behavior can be drawn from the variation in the total organic content. In general, a rising TOC content typically corresponds to the transgressive systems tracts with peak values slightly above the maximum flooding surface. Lower TOC values are associated with the lowstand systems tract and the late (regressive) highstand systems tract. The very low TOC contents (below 0.25 wt%) in sequence 4 may indicate effective shutoff of terrigeneous input (Ricken, 1996).

Sequence architecture

The maximum environmental shift during deposition of a sedimentary sequence, as identified from component lithofacies, defines the magnitude of the sedimentary sequence ("maximum shift of facies", see Yang and Kominz, 2002). This magnitude is an indicator of the maximum shoreline movement relative to a site and can be used to characterize a sequence to aid in its correlation, as well as to constrain the magnitude of related sea-level changes.

During the lowstand and transgressive interval, progradational parasequences composed of sandy bioclastic packstone (e.g., *Turritella* Rock) accumulated in shallow, inner neritic settings. These carbonate accumulations were eventually drowned and buried by silty claystones when rapidly increased water depth hindered (macrofossil) carbonate productivity and depositional energy was lowered. During the subsequent highstand systems tract, carbonate production dominated on the middle to outer shelf but was diluted by influx of terrigeneous detritus (clay and silt), resulting in the accumulation of silty and marly carbonates (e.g., during the HST of the Pine Barren Member). During the late regressive highstand, rapid

shallowing and increased terrigeneous supply subdued largely carbonate productivity.

This sequence pattern may be indicative of 'reciprocal' sedimentation, reflecting a marked 'partitioning' in the dominant sediment type and deposition style with respect to relative sea-level behavior (Southgate et al., 1993; Wright and Burchette, 1996). Studies of such mixed systems suggest that carbonate sedimentation prevails during relative sea-level rises and highstands, while siliciclastic sedimentation dominates during lowstands when carbonate production is largely shut down (Southgate et al., 1993; Wright and Burchette, 1996), an observation that is in keeping with the data from the Antioch Church core.

Considering the magnitude of changes in the depositional environment of the Antioch Church core, lithofacies changes are mostly associated with shifts from inner to middle shelf settings. The presence of vadose marine cements and incipient soil formation atop of the *Turritella* Rock, suggests a brief interval of significant shoaling with temporary emersion. However, this evidence is restricted to this particular sequence in the Antioch Church core, and has not been observed in the sequences below and above. In addition, there is no indication for estuarine or fluvially induced deposits in the Antioch Church core. The sandstone intervals (e.g., the Clayton Basal Sands) generally contain marine fossils, as well as glaucony and are therefore referred to as marine sands. Also, in the sandy bioclastic limestones, fossils appear to be reworked from nearshore settings (e.g., algae) and the large grain size of the constituents suggests a high-energy environment, probably above storm wave or even wave base (i.e., <25 m). On the other hand, evidence for water depths exceeding those typical of inner to middle shelf deposits has not been found (Baum and Vail, 1988), and according to Mancini and Tew (1993), such outer shelf deposits are not represented anywhere in the upper Cretaceous to lower Paleogene strata of central Alabama. The condensed claystone intervals around the maximum flooding surfaces may have been deposited below storm wave base, probably in a water depth exceeding 30 m as inferred from studies at the nearby Braggs outcrop (Baum and Vail, 1988; Donovan et al., 1988). For the silty claystone intervals in the upper highstand systems tract, immediate below the sequence boundary, it is difficult to assign a distinct water depth range, though the poor macrofaunas and the absence of planktic foraminifera may tentatively suggest a shallow water depth, in-between 20-40 m, which is in the range given by Olsson et al. (1996) for the upper part of the Prairie Bluff Fm at Millers Ferry. In conclusion, these observations suggest that changes of the depositional environment operated for the most part within marine settings and, there, within a rather small range.

Foraminifera and paleodepth

In general, the foraminiferal data indicate rather shallow inner to middle neritic deposition at Antioch Church. The number of planktic specimens rarely reaches 10% and usually ranges between 0 and 5%. In modern shelf environments, such low planktic/benthic (P/B) ratios are indicative of deposition at depths not exceeding 50 m. For the Maastrichtian to Paleocene low-to-middle-latitude shelves it was probably even less, considering that P/B ratios of shelf deposits were generally much higher than today. For instance, P/B ratios of the Tethyan outer neritic realm often contain well above 90% planktics (Speijer and Van der Zwaan, 1996; Speijer and Schmitz, 1998; Speijer, 2003). In modern environments, such values indicate depths of around 1000 m (Van der Zwaan et al., 1990), but in the Maastrichtian to Paleocene, deposition at these shelves was probably not deeper than 200-300 m. Similarly, the Brazos area, which was estimated to have been 50-100 m deep at K-P boundary time, yields foraminiferal assemblages with 50-90% planktics (Schulte et al., 2006).

The Paleocene assemblages represent the well-known Midway-type assemblage (Berggren and Aubert, 1975), indicative of neritic deposition during the Paleocene. The taxa observed are common at depths <50 m, although individual taxa may also occur at outer neritic depths or even bathyal deposits (Berggren and Aubert, 1975). Fluctuations in diversity associated with fluctuations in P/B ratios suggest subtle changes in water depth, e.g. ranging between 20 and ~40 m. Shallowest conditions were reached during deposition of the Clayton Basal Sands as revealed by the near absence of planktics. The overlying lower part of the Pine Barren Member contains assemblages that are more diverse and show higher P/B ratios (5-10% planktics), pointing to an overall increasing paleodepth, although deposition of the uppermost HST of the Pine Barren Member (35 to 45 in core depth) with almost zero planktics terminated this general trend. The *Turritella* Rock and the McBryde Limestone Member, however, include a slight amount of planktics though the poor preservation of foraminifera in these units hampers a firmer interpretation of depositional conditions by means of foraminifera.

Depositional depths of the Maastrichtian Prairie Bluff Fm are more difficult to constrain, because the depth distribution of the observed taxa is not well known. Some of the taxa encountered occur in the paleoslope model of Olsson and Nyong (1984), but the majority was apparently not present in the New Jersey transect where this model was developed. Some of the taxa that are common in the New Jersey transect (*Coryphostoma plaita* and *C. incrassata*), occur at depths exceeding 100 m. Such depths are

well beyond any realistic range considering the low P/B ratios and the inner to middle neritic sedimentary facies for the strata of the Antioch Church core. Clearly, these taxa must have occupied shallower habitats in Alabama. This of course greatly inhibits the practical use of depths ranges from one basin to another. On the other hand, there is a fair resemblance of Antioch Church benthic foraminifera with the Prairie Bluff assemblages encountered at Millers Ferry (Olsson et al., 1996), though some common taxa at Millers Ferry such as *Cibicides harperi*, *Anomalinoides praeacutus* are absent at Antioch Church, whereas *Cibicides succedens*, and *Anomalinoides aff. acutus* were not encountered at Millers Ferry. In addition, many slender taxa with an endobenthic morphology observed at Millers Ferry, such as *Pseudouvigerina seligi* and *Tappanina selmensis* were rarely encountered at Antioch Church. This is clearly a result from the different size fractions used: >125 μm in our study and >63 μm in the study by Olsson et al., 1996; and Olsson pers. comm. 2006. The Prairie Bluff fauna at Millers Ferry contains a slightly different benthic assemblage and more numerous planktic specimens. This suggests that Antioch Church was shallower than Millers Ferry, which is in agreement with an offshore position for Millers Ferry as indicated by the facies distribution in Alabama during the Maastrichtian (Donovan et al., 1988; Olsson et al., 1996). In conclusion, we estimate water depths between 20-40 m during deposition of the Prairie Bluff Fm, with deposition towards the deeper end of this range in the uppermost two meters and towards the shallower range in the lower part of the studied part of the succession.

Regional and global correlation of sequences

Preconditions for the correlation of sequence boundaries and the succession of systems tracts between coeval marine sections are: a precise identification of the corresponding sequence stratigraphic surfaces and a tight chronostratigraphic framework. Both criteria are, however, difficult to establish for the Antioch Church core because of:

1) The different behavior of the sedimentary system in response to changes in proximity of the shoreline, detrital input, and/or paleobathymetry: In the siliciclastic-dominated part, the sedimentary system acts in a more 'robust' way, with a range of intermediate lithologies (e.g., marls), whereas the carbonate-dominated system shows, almost, a bimodal distribution of lithofacies with rapid 'give-up' of the carbonate production. This has also been interpreted as 'reciprocal' sedimentary pattern (Southgate et al., 1993; Strasser et al., 1999).

2) According to examples from mixed carbonate-siliciclastic systems (Strasser et al., 1999; Sanders and Höfling, 2000; Yang and Kominz, 2002), carbonate-rich facies tend to occur in a diverse patch-like distributed pattern on the shelf ("compartmentalization"), with intermittent areas of mainly siliciclastic sedimentation. Hence, a vertical succession must be established within a regional framework to distinguish changes produced by local facies shifts from regional sea-level trends.

3) The biostratigraphic control makes it difficult to assign a biostratigraphic age to the enclosed sequence stratigraphic surfaces (Fig. 2). Sequence stratigraphic surfaces occur either during nannofossil zones and/or coincide with first/last occurrences of zonal marker fossils. In addition, these sequence stratigraphic surfaces are often associated with an unconformity at which a hiatus (possibly subaerial exposure) of unknown duration exists. This problem was recognized by Baum and Vail (Baum and Vail, 1988) and they concluded that a sequence boundary must not be dated at their upper shelf extension (i.e., the setting of the Antioch Church core), but rather in deeper marine settings at their 'correlative conformity', to obtain reliable age estimates.

4) Flooding and maximum flooding 'surfaces' are difficult to tie to 'discrete' lithologic surfaces, but instead enclose a distinct (condensed) sedimentary interval, usually 10-40 cm in thickness in the Antioch Church core (see Fig. 3). The same applies to the late highstand intervals, during which relative sea level was probably lowest and terrigeneous input at maximum – these intervals have usually gradual transitions to the underlying deposits of the highstand – complicating the assignation of a point in time referred to as "lowstand".

This excursion highlights the problems in dating sequence stratigraphic surfaces in the shallow shelf setting of the Antioch Church core and consequently, it is difficult to assign particular age constraints based on biostratigraphy to these surfaces. Specifically, for the upper Maastrichtian strata of the Antioch Church core, which revealed a distinct lowering of water depth during progradational highstand conditions associated with increased siliciclastic input (between about 70 to 75 m in core depth), it is not possible to give a reasonable 'timing' for this lowering of relative sea level, other than that it occurred somewhere during the upper part of Biozones CC25 / CF3. Therefore, this sea level lowering may have occurred during the interval from 600 to 300 ky preceding the K-P boundary. This unclear timing makes any comparison to published sea-level charts impossible.

For the K-P transition and the lower Danian, the Haq et al. (1988) sea-level chart shows a transgressive interval. Erikson and Pindell (1998) suggest a minor lowstand extending across the K-P boundary, followed by gradually

rising sea level in the early Danian. Hardenbol and Robaszynski (1998), show a sea-level lowstand at the K-P boundary followed by two minor sequences in the lower Danian, with sequence boundaries dated at 64.6 Ma (Da1; middle part of NP1), 64 Ma (Da2, middle part of NP2; Neal and Hardenbol, 1998). The curves provided by Miller et al. (2005) and Olsson et al. (2002) show slight lowering of sea level across the K-P boundary, followed by transgression during the earliest Danian. Similarly, the sedimentary records of the Antioch Church core shows evidence for a lowstand at or close to the K-P boundary followed by a transgressive trend, which culminated during the lowermost Danian up to about 0.5 My post K-P (maximum flooding surface in upper part of Biozone NP1), and which was followed by a highstand systems tract during Biozone NP2.

The sequence stratigraphy of the middle to upper Danian was compiled by Neal and Hardenbol (1998) and revealed a sequence boundary at 63 Ma (Da3; middle part of NP3), and a sequence boundary in the upper Danian at 61.5 Ma (Da4; middle part of NP4). In contrast, the Haq et al. (1988) curve contains only one major lowstand at 63 Ma, which corresponds approximately to the Da3 sequence boundary. The sea level curves provided by Miller et al. (2005) and Olsson et al. (2002) reveal rapid rise in sea level with a high-magnitude (>50 m) during the middle Danian, approximately at the Biozone P1b/P1c boundary. The middle and upper Danian strata in the Antioch Church core, however, show two sequence boundaries during this period, with more pronounced changes in the water depth than recorded in the lower Danian sediments. One sequence boundary is situated in the upper part of Biozones NP2 / P1a, whereas the second sequence boundary is positioned within Biozone NP3/ P1c. However, a switch of the depositional system (from siliciclastic to mixed-siliciclastic-carbonate), and the different behavior of the sedimentary system in response to water depth or proximity changes both make an evaluation difficult.

As a bottom line, it appears that the derivation of an affirmative global curve is currently in flux and, with the, in part contradictory sea-level trends derived from the literature data for this period, it would be possible to make a correlation of the sequence boundaries and sea-level trends derived from the Antioch Church core, with some of those proposed in these studies. Consequently, no constraints for global correlation are inferred from the data obtained during this study.

The K-P boundary event bed

The Clayton Basal Sands consists of a one-meter thick, moderately to poorly sorted, faintly normal graded sandstone body with a pyritized base that overlies the sandy marls of the uppermost Prairie Bluff Fm. Its upper part shows slight lamination, and bioturbation is not present. Therefore, this sandstone is interpreted to reflect rapid deposition under high-energy traction transport as debris flow with waning-flow conditions preserved at the laminated top (Mulder and Alexander, 2001). These characteristics qualify this sandstone to be considered an event bed (Einsele, 1998).

The pyrite-rich sandstone layer intercalated between the Prairie Bluff and the Clayton Basal Sands is, with exception of the pyritized matrix, compositionally similar to the Clayton Sands above, but is totally devoid of carbonate or fossil tests. Bulk rock X-ray diffractometry showed the additional presence of goethite and jarosite. Jarosite is a potassium-iron-sulfate that forms by weathering of organic-rich sediments by oxidization of pyrite, which produces sulfuric acid that attacks illite and K-feldspar, and liberates potassium (Moore and Reynolds, 1997). Hence, jarosite and goethite may indicate increased organic matter associated with deposition of the sandstone and/or a subsequent period of anoxic conditions that both promoted the formation of pyrite. Suboxic or anoxic conditions may also be suggested by elevated Cu (40 ppm), As (300 ppm), and Pb (35 ppm) concentrations, compared to the enclosing lithologies (Tribovillard et al., 2000). Moreover, jarosite and goethite are a common component of the marine and terrestrial K-P boundary clay layer (e.g., Schmitz, 1992; Tribovillard et al., 2000; Wdowiak et al., 2001). However, no increased amount of trace elements (e.g., Ni, Cr, Co) that may be linked to extraterrestrial influx was found in the Antioch Church core.

The petrography of the Clayton Basal Sands suggests derivation from shore-nearshore, shallow-water areas with concomitant admixture of ejecta-fallout material. During high-energy transport, winnowing may have been intense and led to the comprehensive removal of fine-grained detritus. Events capable of generating such deposits are usually storms or tsunamis, which may create intense offshore-directed backflows through buildup of water masses along the coast (Myrow and Southard, 1996; Einsele, 1998; Dawson and Shi, 2000). These strong backflow currents may transport large quantities of sand towards outer shelf areas. The triggering cause(s) of these events is, however, difficult to constrain from the limited data of a cored section. The presence of ejecta spherules, however, suggests that deposition occurred subsequently to ejecta fallout from the Chicxulub impact at the Yucatán peninsula in southern Mexico.

In summary, an origin by a short-lived depositional event is concluded for the Clayton Basal Sands in the

Antioch Church core, instead of aggradation during long periods. This interpretation is in line with observations from other K-P sections in the Gulf Coast plain of Alabama where a chaotic sandstone bed with reworked Prairie Bluff chalk clasts at the base of the Clayton Sands has been considered as event deposits associated with high current energies and deposition of chaotic boulder (>1 m in diameter!) beds (e.g., at Moscow Landing Habib et al., 1996; Olsson et al., 1996; Smit et al., 1996). In contrast, our lithological and petrological data, as well as lithological data provided by Savrda (1993) and Olsson et al. (1996) shows that the upper part of the Clayton Basal Sands in the Mussel Creek and Millers Ferry outcrops is thinly bedded, highly micaceous, strongly bioturbated, contains no Chicxulub ejecta material, and is entirely Paleocene in age (Biozone Pα). Therefore, the observations by Savrda (1993) in support of long-term deposition of the upper Clayton Basal Sands in the nearby Mussel Creek K-P section as well by Olson et al. (1996) for the Millers Ferry outcrop may be explained by the different lithological nature and stratigraphic setting of these sandstone beds, compared to Clayton Basal Sands in the Antioch Church core.

The comparison to the Mussel Creek and Millers Ferry K-P sections therefore may also shed light on the problems for constraining the depositional nature of the K-P sections in Alabama: namely, that the Clayton Basal Sands show different lithological characteristics and even distinctive depositional ages in different outcrops (Mancini and Tew, 1993). Consequently, a unique or single-event origin for the K-P boundary deposits in Alabama is not justified by the sedimentological data and various causes may be responsible for their origin (storms, tsunamis, sea-level fluctuations).

Clay mineralogy and paleoclimate

The diversity of clay mineral assemblages identified in the sediments of the Antioch Church core may reflect either a detrital or a diagenetic origin. For that reason, evaluation of these clay mineral assemblages with respect to paleoenvironmental signals first requires investigation and assessment of diagenetic features. However, the sediments of the Antioch Church core did not suffer deep burial (at maximum several hundred meters) and there is no concomitant increase in illite-smectite, illite, and chlorite that each would indicate smectite transformation to chlorite and illite during burial diagenesis (Chamley, 1997). Moreover, a low burial diagenetic overprint throughout the Antioch Church core is documented by the co-existence of smectite with high kaolinite content. Since most of these clay minerals, including kaolinite, illite, and chlorite are not very sensitive to slight or moderate depths of burial (Chamley, 1997), and since clay minerals in the Alabama Gulf coast region were apparently not affected by volcano-hydrothermal activity, the clay mineral facies of the Antioch Church core are mainly considered to be detrital in origin, though minor smectite authigenesis may have occurred in sandy intervals. The clay mineral assemblage therefore reflects processes taking place in their source area or processes associated with their transport path.

Clay minerals in the Antioch Church core show a prominent change from a late Maastrichtian kaolinite-dominated to middle Danian smectite-dominated assemblage. The gradual nature of this change, almost independent of lithology and position in the sequence stratigraphic framework, suggests an inherited signal of proximity to the shoreline without larger influx. Therefore, this clay mineral succession may be interpreted as a change from almost tropical climates with high year-round precipitation and percolation to subtropical to semiarid climates with lower precipitation, usually seasonal, and lower water percolation (Chamley, 1997; Gibson et al., 2000). Following Gibson et al. (2000), such a climate change may also be associated with a general temperature decrease. However, the lack of detailed clay mineral as well as stable isotope studies from the Alabama Gulf coast province for this period prevents from evaluation of these climatic trends within a regional context. Such an evaluation and comparison could give evidence whether a shift in regional climates happened, or if these changes were associated with local changes in the depositional system.

CONCLUSIONS

In the sediments of the Antioch Church core, a trend is recognized from a siliciclastic-dominated depositional system in the late Maastrichtian-early Danian, to a mixed siliciclastic-carbonate depositional system during the middle Danian. This change may be related to the establishment of a stable carbonate platform on the Alabama shelf during the early Paleocene, as shown by Mancini and Tew (1993).

Four depositional sequences were distinguished for the late Maastrichtian to upper Danian period. In this mixed depositional system on the Alabama shelf, siliciclastic sedimentation dominated during the late (regressive) highstand and subsequent lowstand systems tracts, when carbonate production was largely shut down. Carbonate sedimentation prevailed during the transgressive and the early highstand systems tracts, when terrigeneous detritus was mostly trapped in nearshore areas. This vertical stacking pattern is known as “reciprocal sedimentation” (Southgate et al., 1993).

The vertical succession of component lithofacies suggests that the magnitude of relative sea-level changes was largest during the middle Danian sequences (temporal emergence), whereas magnitudes are less pronounced during the late Maastrichtian-early Danian and the upper Danian sequences.

The changes in terrigeneous input and energy-level during a sequence are reflected by characteristic changes in the major and trace element, as well as in specific element ratios and the TOC content of the sediments. Along with the gamma-ray log response, these geochemical data allow for monitoring facies changes and a detailed internal subdivision of the depositional sequence.

At the K-P boundary, a siliciclastic event bed is intercalated within a transgressive systems tract and contains ejecta spherules that are morphologically similar to ejecta from the Chicxulub impact found in K-P sections from the Gulf of Mexico area, and the K-P boundary clay in Northern America (Western Interior), the Western Atlantic, and the Pacific. The depositional nature of the K-P event bed is difficult to constrain from the Antioch Church core, and tsunami- or storm-triggered mechanisms are possible, whereas formation as an incised valley fill is not compatible with the sedimentological characteristics of this bed.

Clay minerals of the Antioch Church core comprise mainly varying proportions of smectite, kaolinite, and illite. Three distinct clay mineral facies were distinguished: (i) a kaolinite-dominated facies with a general upward increase in the relative abundance of smectite concomitant to a relative decrease in kaolinite, (ii) a kaolinite-smectite-rich facies, and (iii) a smectite-illite-dominated facies. The latter facies was established at the transition to a carbonate-dominated sedimentary system.

The general trends in clay mineral abundances are not exclusively related to lithological changes, though minor compositional changes occur at lithologic transitions and coincident to sequence stratigraphic surfaces. However, the overall variations in clay mineral assemblages likely resulted mainly from paleoclimate variations in the source area and only to a minor degree from the position relative to the coastline. This climate change may have included a change from humid conditions with year-round precipitation to semiarid climates with pronounced seasonality.

ACKNOWLEDGEMENTS

Very special thanks go to Gerald Baum for access to the AC core, core photos, and support as well as for a great introduction to sequence stratigraphy! Wolfgang Stinnesbeck (University Karlsruhe, Germany), Thierry Adatte (University Neuchâtel, Switzerland), Doris Stüben, and Utz Kramar (both Karlsruhe University) are acknowledged for support and help with the mineralogical and geochemical analysis. In addition, Hartmut Mai (University Bremen, Germany) is greatly acknowledged for contributing the calcareous nannofossil stratigraphy. We are also indebted to the editorial handling by Victoriano Pujalte as well as to the constructive suggestions by the reviewers Ernest A. Mancini, Richard K. Olsson, and Henning Dypvik that significantly helped improving the manuscript.

REFERENCES

Adatte, T., Keller, G., Stinnesbeck, W., 2002. Late Cretaceous to early Paleocene climate and sea-level fluctuations: The Tunisian record. Palaeogeography, Palaeoclimatology, Palaeoecology, 178(3-4), 165-196.

Alonso Zarza, A.M., Sanz, M.E., Calvo, J.P., Estevez, P., 1999. Calcified root cells in Miocene pedogenic carbonates of the Madrid Basin: Evidence for the origin of Microcodium b. Sedimentary Geology, 116(1-2), 81-97.

Amorosi, A., 1995. Glaucony and sequence stratigraphy: A conceptual framework of distribution in siliciclastic sequences. Journal of Sedimentary Research, B65(4), 419-425.

Baum, G.R., Vail, P.R., 1988. Sequence stratigraphic concepts applied to Paleogene outcrops, Gulf and Atlantic basins. In: Wilgus, C.K., Hastings, B.S., Kendall, C.G., Posamentier, H.W., Ros, C., Van Wagoner, J.C. (eds.). Sea-level changes: An integrated approach. Tulsa, Oklahoma, Society of Economic Paleontologists and Mineralogists, Special Publication, 42, 309-327.

Berggren, W.A., Aubert, J., 1975. Paleocene benthonic foraminiferal biostratigraphy, paleobiogeography and paleoecology of Atlantic-Tethyan regions: Midway-type fauna. Palaeogeography, Palaeoclimatology, Palaeoecology, 18(2), 73-192.

Berggren, W.A., Kent, D.V., Swisher, C.C., Aubry, M.-P., 1995. A revised Cenozoic geochronology and chronostratigraphy. In: Berggren, W.A., Kent, D.V., Aubry, M.-P., Hardenbol, J. (eds.). Geochronology, time scales, and global stratigraphic correlation. Tulsa, Oklahoma, Society of Economic Paleontologists and Mineralogists, Special Publication, 54, 129-212.

Berggren, W.A., Norris, R.D., 1997. Biostratigraphy, phylogeny and systematics of Paleocene trochospiral planktonic foraminifera. Micropaleontology, 43, Suppl. 1, 1-116.

Biscaye, P.E., 1965. Mineralogy and sedimentation of recent deep-sea clay in the Atlantic Ocean and adjacent seas and oceans. Geological Society of America Bulletin, 76(7), 803-832.

Bohor, B.F., Glass, B.P., 1995. Origin and diagenesis of K/T impact spherules – From Haiti to Wyoming and beyond. Meteoritics, 30, 182-198.

Chamley, H., 1997. Clay mineral sedimentation in the ocean. In: Paquet, H., Clauer, N. (eds.). Soils and sediments. Heidelberg, Germany, Springer, 269-302.

Dawson, A.G., Shi, S., 2000. Tsunami deposits. Pure and Applied Geophysics, 157(6-8), 875-897.

Donovan, A.D., Baum, G.R., Blechschmidt, G.L., Loutit, T.S., Pflum, C.E., Vail, P.R., 1988. Sequence stratigraphic setting of the Cretaceous-Tertiary boundary in central Alabama. In: Wilgus, C.K., Hastings, B.S., Kendall, C.G., Posamentier, H.W., Ros, C., Van Wagoner, J.C. (eds.). Sea-level changes: An integrated approach. Tulsa, Oklahoma, Society of Economic Paleontologists and Mineralogists, Special Publication, 42, 299-307.

Dypvik, H., Harris, N.B., 2001. Geochemical facies analysis of fine-grained siliciclastics using Th/U, Zr/Rb and (Zr+Rb)/Sr ratios. Chemical Geology, 181(1-4), 131-146.

Einsele, G., 1998. Event stratigraphy: Recognition and interpretation of sedimentary event horizons. In: Doyle, P., Bennet, M. (eds.). Unlocking the stratigraphical record: Advances in modern stratigraphy. New York, John Wiley and Sons, 145-194.

Erikson, J.P., Pindell, J.L., 1998. Sequence stratigraphy and relative sea-level history of the Cretaceous to Eocene passive margin of northeastern Venezuela and the possible tectonic and eustatic causes of stratigraphic development. In: Pindell, J.L., Drake, C.L. (eds.). Paleogeographic evolution and non-glacial eustasy, northern South America. Tulsa, Oklahoma, Society of Economic Paleontologists and Mineralogists, Special Publication, 58, 261-281.

Garcia, D., Pascal, M.L., Roux, J., 1996. Hydrothermal replacement of feldspars in igneous enclaves of the Velay granite and the genesis of myrmekites. European Journal of Mineralogy, 8, 703-717.

Gardin, S., 2002. Late Maastrichtian to early Danian calcareous nannofossils at Elles (Northwest Tunisia): A tale of one million years across the K/T boundary. Palaeogeography, Palaeoclimatology, Palaeoecology, 178(3-4), 211-231.

Gartner, S., 1996. Calcareous nannofossils at the Cretaceous-Tertiary boundary. In: MacLeod, N., Keller, G. (eds.). Cretaceous-Tertiary boundary mass extinction: Biotic and environmental changes. New York, Norton Press, 27-48.

Gibson, T.G., Bybell, L.M., Mason, D.B., 2000. Stratigraphic and climatic implications of clay mineral changes around the Paleocene/Eocene boundary of the northeastern US margin. Sedimentary Geology, 134, 65-92.

Habib, D., Olsson, R.K., Liu, C., Moshkovitz, S., 1996. High-resolution biostratigraphy of sea-level low, biotic extinction, and chaotic sedimentation at the Cretaceous-Tertiary boundary in Alabama, north of the Chicxulub crater. In: Ryder, G., Fastovsky, D., Gartner, S. (eds.). The Cretaceous-Tertiary boundary event and other catastrophes in Earth history. Boulder, Colorado, Geological Society of America, Special Paper, 307, 243-252.

Hampson, G.J., Davies, W., Davies, S.J., Howell, J.A., Adamson, K.R., 2005. Use of spectral gamma-ray data to refine subsurface fluvial stratigraphy: Late Cretaceous strata in the Book Cliffs, Utah, USA. Journal of the Geological Society, London, 164(4), 603-621.

Haq, B.U., Hardenbol, J., Vail, P.R., 1988. Mesozoic and Cenozoic chronostratigraphy and cycles of sea-level change. In: Wilgus, C.K., Hastings, B.S., Kendall, C.G., Posamentier, H.W., Ros, C. (eds.). Sea-level changes: An integrated approach. Tulsa, Oklahoma, Society of Economic Paleontologists and Mineralogists, Special Publication, 42, 71-108.

Hardenbol, J., Robaszynski, F., 1998. Introduction to the Upper Cretaceous. In: de Graciansky, P.-C., Hardenbol, J., Jacquin, T., Vail, P.R. (eds.). Mesozoic and cenozoic sequence stratigraphy of European basins. Tulsa, Oklahoma, Society of Economic Paleontologists and Mineralogists, Special Publication, 60, 329-332.

Jones, D.S., Mueller, P.A., Bryan, J.R., Dobson, J.P., Channell, J.E.T., Zachos, J.C., Arthur, M.A., 1987. Biotic, geochemical and paleomagnetic changes across the Cretaceous/Tertiary boundary at Braggs, Alabama. Geology, 15(4), 311-315.

Kramar, U., 1997. Advances in energy-dispersive X-ray fluorescence. Journal of Geochemical Exploration, 58, 73-80.

Langford, F.F., Blanc-Valleron, M.-M., 1990. Interpreting Rock-Eval pyrolysis data using graphs of pyrolizable hydrocarbons vs. total organic carbon. AAPG Bulletin, 74(6), 799-804.

Mancini, E.A., Tew, B.H., 1993. Eustasy versus subsidence: Lower Paleocene depositional sequences from southern Alabama, eastern Gulf Coastal Plain. Geological Society of America Bulletin, 105(1), 3-17.

Mancini, E.A., Puckett, T.M., Tew, B.H., 1996, Integrated biostratigraphic and sequence stratigraphic framework for Upper Cretaceous strata of the eastern Gulf Coastal Plain, USA. Cretaceous Research, 17(6), 645-669.

Mancini, E.A., Tew, B.H., 1997. Recognition of maximum flooding events in mixed siliciclastic-carbonate systems: Key to global chronostratigraphic correlation. Geology, 25(4), 351-354.

Martini, E., 1971. Standard Tertiary and Quarternary calcareous nannoplankton zonation. In: Farinacci, A. (ed.). Second International Planktonic Conference Proceedings, Rome, Technoscienza, 739-785.

Miller, K.G., Kominz, M.A., Browning, J.V., Wright, J.D., Mountain, G.S., Katz, M.E., Sugarman, P.J., Cramer, B.S., Christie-Blick, N., Pekar, S.F., 2005. The Phanerozoic record of global sea-level change. Science, 310, 1293-1298.

Moore, D.M., Reynolds, R.C., 1997. X-ray diffraction and the identification and analysis of clay minerals. Oxford, Oxford University Press, 378 pp.

Moshkovitz, S., Habib, D., 1993. Calcareous nannofossil and dinoflagellate stratigraphy of the Cretaceous-Tertiary boundary, Alabama and Georgia. Micropaleontology, 39(2), 167-191.

Mulder, T., Alexander, J., 2001. The physical character of subaqueous sedimentary density flows and their deposits. Sedimentology, 48(2), 269-299.

Myrow, P.M., Southard, J.B., 1996. Tempestite deposition. Journal of Sedimentary Research, 66(5), 861-866.

Neal, J.E., Hardenbol, J., 1998. Introduction to the Paleogene. In: de Graciansky, P.-C., Hardenbol, J., Jacquin, T., Vail, P.R. (eds.). Mesozoic and Cenozoic sequence stratigraphy of European basins. Tulsa, Oklahoma, Society of Economic Paleontologists and Mineralogists, Special Publication, 60, 87-90.

Olsson, R.K., Liu, G., 1993. Controversies on the placement of the Cretaceous-Paleogene boundary and the K/T mass extinction of planktonic foraminifera. Palaios, 8, 127-139.

Olsson, R.K., Nyong, E.E., 1984. A paleoslope model for Campanian–lower Maastrichtian foraminifera of New Jersey and Delaware. Journal of Foraminiferal Research, 14(1), 50-68.

Olsson, R.K., Liu, C., van Fossen, M., 1996. The Cretaceous-Tertiary catastrophic event at Millers Ferry, Alabama. In: Ryder, G., Fastovsky, D., Gartner, S. (eds.). The Cretaceous-Tertiary boundary event and other catastrophes in Earth history. Boulder, Colorado, Geological Society of America, Special Paper, 307, 263-277.

Olsson, R.K., Hemleben, C., Berggren, W.A., Huber, B.T. (eds.), 1999. Atlas of Paleocene planktonic foraminifera. Smithsonian contributions to Paleobiology, 85, 254 pp.

Olsson, R.K., Miller, K.G., Browning, J.V., Wright, J.D., Cramer, B.S., 2002. Sequence stratigraphy and sea-level changes across the Cretaceous-Tertiary boundary on the New Jersey passive margin. In: Koeberl, C., MacLeod, K.G. (eds.). Catastrophic events and mass extinctions: Impacts and beyond. Boulder, Colorado, Geological Society of America, Special Paper, 356, 97-108.

Pardo, A., Ortiz, N., Keller, G., 1996. Latest Maastrichtian and Cretaceous-Tertiary foraminiferal turnover and environmental changes at Agost, Spain. In: MacLeod, N., Keller, G. (eds.). Cretaceous-Tertiary boundary mass extinction: Biotic and environmental changes. New York, Norton Press, 139-171.

Perch-Nielsen, K., 1985. Mesozoic calcareous nannofossils. In: Saunders, J.B., Bolli, H.M., Perch-Nielsen, K. (eds.). Plankton stratigraphy. Cambridge, United Kingdom, Cambridge University Press, 329-426.

Petschick, R., Kuhn, G., Gingele, F.X., 1996. Clay mineral distribution in surface sediments of the South Atlantic: Sources, transport, and relation to oceanography. Marine Geology, 130(3-4), 203-229.

Ricken, W., 1996. Bedding rhythms and cyclic sequences as documented in organic carbon-carbonate patterns, Upper Cretaceous, Western Interior, USA. Sedimentary Geology, 102(1-2), 131-154.

Rider, M.H., 1996. The geological interpretation of well logs. Caithness, United Kingdom, Whittles Publishing, 361 pp.

Sanders, D., Höfling, R., 2000. Carbonate deposition in mixed siliciclastic-carbonate environments on top of an orogenic wedge (Late Cretaceous, Northern Calcareous Alps, Austria). Sedimentary Geology, 137(3-4), 127-146.

Savrda, C.E., 1991. Ichnology in sequence stratigraphy: An example from the Lower Paleocene from Alabama. Palaios, 6(1), 39-53.

Savrda, C.E., 1993. Ichnosedimentologic evidence for a noncatastrophic origin of Cretaceous-Tertiary boundary sands in Alabama. Geology, 21(12), 1075-1078.

Schmitz, B., 1992. Chalcophile elements and Ir in continental Cretaceous-Tertiary boundary clays from the Western Interior of the USA. Geochimica et Cosmochimica Acta, 56(4), 1695-1703.

Schulte, P., Kontny, A., 2005. Chicxulub ejecta at the Cretaceous-Paleogene (K-P) boundary in Northeastern México. In: Hörz, F., Kenkmann, T., Deutsch, A. (eds.). Large meteorite impacts III. Boulder, Colorado, Geological Society of America, Special Paper, 384, 191-221.

Schulte, P., Speijer, R.P., Mai, H., Kontny, A., 2006. The Cretaceous-Paleogene (K-P) boundary at Brazos, Texas: Sequence stratigraphy, depositional events and the Chicxulub impact. Sedimentary Geology, 184(1-2), 77-109.

Smit, J., Alvarez, W., Montanari, A., Claeys, P., Grajales-Nishimura, J.M., 1996. Coarse-grained, clastic sandstone complex at the K/T boundary around the Gulf of Mexico: Deposition by tsunami waves induced by the Chicxulub impact? In: Ryder, G., Fastovsky, D., Gartner, S. (eds.). The Cretaceous-Tertiary boundary event and other catastrophes in Earth history. Boulder, Colorado, Geological Society of America, Special Paper, 307, 151-182.

Sohl, N.F., Martínez, E.R., Salmerón-Ureña, P., Soto-Jaramillo, F., 1991. Upper Cretaceous. In: Salvador, A. (ed.). The Gulf of Mexico Basin. The geology of North America, J, Boulder, Colorado, Geological Society of America, 205-244.

Southgate, P.N., Kennard, J.M., Jackson, M.J., O'Brian, P.E., Sexton, M.J., 1993. Reciprocal lowstand clastic and highstand carbonate sedimentation, subsurface Devonian Reef complex, Canning Basin, Western Australia. In: Loucks, R.G., Sarg, J.F. (eds.). Carbonate sequence stratigraphy: Recent developments and applications. Tulsa, Oklahoma, American Association of Petroleum Geologists, Memoir, 57, 157-179.

Speijer, R.P., 2003. Danian-Selandian sea-level change and biotic excursion on the southern Tethyan margin (Egypt). In: Wing, S.L., Gingerich, P.D., Schmitz, B., Thomas, E. (eds.). Causes and consequences of globally warm climates in the early Paleogene. Boulder, Colorado, Geological Society of America, Special Paper, 369, 275-290.

Speijer, R.P., Schmitz, B., 1998. A benthic foraminiferal record of Paleocene sea level and trophic/redox conditions at Gebel Aweina, Egypt. Palaeogeography, Palaeoclimatology, Palaeoecology, 137(1-2), 79-101.

Speijer, R.P., Van der Zwaan, G.J., 1996. Extinction and survivorship of southern Tethyan benthic foraminifera across the Cretaceous/Paleogene boundary. In: Hart, M.B. (ed.). Biotic recovery from mass extinction events. Geological Society, London, Special Publication, 102, 343-371.

Strasser, A., Pittet, B., Hillgaertner, H., Pasquer, J.-B., 1999. Depositional sequences in shallow carbonate-dominated sedimentary systems: Concepts for a high resolution analysis. Sedimentary Geology, 128(2), 201-221.

Tribovillard, N., Dupuis, C., Robin, E., 2000. Sedimentological and diagenetical conditions of the impact level of the Cretaceous/Tertiary boundary in Tunisia: No anoxia required. Bulletin de la Société Géologique de France, 171(6), 629-636.

Tucker, M.E., Wright, V.P., 1992. Carbonate sedimentology. Oxford, Blackwell Science, 482 pp.

Van der Zwaan, G.J., Jorissen, F.J., de Stigter, H.C., 1990. The depth dependency of planktonic/benthic foraminiferal ratios: Constraints and applications. Marine Geology, 95(1), 1-16.

Van Wagoner, J.C., Mitchum, R.M., Campion, K.M., Rahmanian, V.D., 1990. Siliciclastic sequence stratigraphy in well logs, cores, and outcrops: Concepts for high-resolution correlation of time and facies. Tulsa, Oklahoma, American Association of Petroleum Geologists, Methods in Exploration, 7, 53 pp.

Wdowiak, T.J., Armendarez, L.P., Agresti, D.G., Wade, M.L., Wdowiak, Y.S., Claeys, P., Izett, G.A., 2001. Presence of an iron-rich nanophase material in the upper layer of the Cretaceous-Tertiary boundary clay. Meteoritics & Planetary Science, 36(1), 123-133.

Wright, V.P., Burchette, T.P., 1996. Shallow-water carbonate environments. In: Reading, H.G. (ed.). Sedimentary environments: Processes, facies and stratigraphy. Oxford, Blackwell Science, 325-394.

Yang, W., Kominz, M.A., 2002. Characteristics, stratigraphic architecture, and time framework of multi-order mixed siliciclastic and carbonate depositional sequences, outcropping Cisco Group (Late Pennsylvanian and Early Permian), Eastern Shelf, north-central Texas, USA. Sedimentary Geology, 154(1-2), 53-87.

Zachos, J.C., Arthur, M.A., Dean, W.E., 1989. Geochemical and paleoenvironmental variations across the Cretaceous/Tertiary boundary at Braggs, Alabama. Palaeogeography, Palaeoclimatology, Palaeoecology, 69, 245-266.

Manuscript received January 2007;
revision accepted March 2008;
published Online October 2008.

APPENDIX

TABLE A1 | **Major and trace element composition of bulk samples from the Antioch Church core by energy-dispersive X-ray fluorescence spectrometry (EDS). All Fe is given as Fe_2O_3.**

AC	Depth	TiO_2	Fe_2O_3	MnO	CaO	K_2O	Cu	Zn	As	Rb	Sr	Y	Zr	Ba	La	Ce	Pb
#	m	wt%	wt%	ppm	wt%	wt%	ppm	ppm	ppm	ppm	ppm	ppm	ppm	ppm	ppm	ppm	ppm
235	1.83	0.18	3.15	266	24.13	1.07	14	94	8	48	459	31	108	182	48	78	<5
232	3.05	0.23	2.99	190	27.79	1.18	8	87	5	47	577	32	149	228	39	56	<5
229	3.96	0.03	0.97	204	47.87	1.31	15	27	<5	<10	577	20	21	26	29	52	<5
226	5.79	0.01	0.33	103	50.10	1.28	<5	11	<5	<10	529	8	12	<5	16	20	<5
223	7.62	0.01	0.61	102	50.16	1.23	8	20	<5	<10	563	11	14	8	21	18	<5
220	9.45	0.01	0.36	61	46.56	1.02	<5	15	<5	<10	455	5	28	70	24	24	<5
217	11.13	0.01	0.64	94	50.26	1.48	<5	17	<5	<10	457	4	10	14	21	22	<5
215	12.04	0.09	2.40	50	40.73	1.36	13	50	<5	27	439	11	43	35	22	35	<5
213	13.41	0.07	2.59	50	39.87	1.16	5	45	<5	28	510	8	26	29	22	24	<5
210	14.78	0.04	0.90	38	45.12	1.05	11	19	<5	10	488	7	35	35	<10	<10	<5
207	16.15	0.36	1.51	64	27.74	1.10	13	32	<5	27	528	14	239	182	26	40	5
205	17.07	0.20	2.23	50	36.21	1.12	9	47	5	31	658	12	86	101	28	50	<5
202	18.68	0.19	1.36	57	39.04	1.02	8	45	<5	20	651	10	96	100	25	36	<5
200	19.20	0.17	2.06	50	37.23	1.25	10	59	<5	29	740	8	44	102	19	34	<5
198	20.57	0.13	1.14	48	42.79	1.02	8	36	<5	17	543	8	53	78	31	40	<5
196	21.49	0.09	0.98	41	43.84	0.85	10	30	<5	13	518	7	51	58	17	21	<5
194	22.40	0.02	0.42	53	49.05	0.89	9	17	<5	<10	533	4	34	40	21	24	<5
192	23.77	0.14	0.75	47	42.34	1.32	11	22	<5	12	503	8	87	62	<10	27	<5
190	24.41	0.29	1.88	50	14.50	1.09	11	48	9	34	698	14	192	259	38	64	<5
188	25.45	0.38	2.50	53	10.53	1.37	13	47	8	42	814	12	188	339	39	63	7
187	25.91	0.32	2.31	50	10.75	1.35	25	52	9	42	858	13	142	375	24	44	6
185	26.67	0.14	1.43	121	32.61	1.40	10	25	<5	16	731	7	58	85	13	29	<5
184	27.22	0.47	3.50	221	22.60	1.16	10	54	8	41	525	17	276	256	30	61	8
182	27.74	0.46	3.05	50	12.94	1.41	11	66	7	55	1004	13	157	292	25	47	7
180	28.41	0.38	2.50	50	10.53	1.37	13	47	8	42	814	12	188	339	39	63	7
179	28.96	0.46	3.77	50	13.39	1.52	11	84	13	60	947	11	111	281	29	57	7
178	29.26	0.42	4.14	50	16.61	1.53	18	90	11	63	838	14	89	232	31	37	9
177	29.41	0.03	1.86	157	47.31	0.76	45	25	73	<10	656	5	24	26	14	<10	<5
176	29.72	0.03	2.09	50	40.14	1.09	12	257	184	<10	574	3	31	44	20	28	5
175	30.33	0.01	1.05	50	39.30	1.11	<5	18	6	<10	464	3	29	37	10	10	<5
173	31.85	0.05	2.54	107	39.81	0.79	18	17	17	7	352	5	43	54	<10	29	<5
171	33.83	0.11	2.57	50	37.07	0.91	<5	18	14	11	329	10	115	78	22	54	5
170	34.59	0.08	1.14	50	38.41	1.02	20	25	7	10	308	11	90	74	17	39	<5
169	35.30	0.06	0.91	173	36.29	0.61	19	19	12	<10	578	7	73	40	13	17	<5
168	35.57	0.63	4.01	50	6.77	1.54	15	61	22	54	337	27	445	319	57	102	13
167	35.81	0.60	3.75	159	7.04	1.52	12	60	37	47	321	21	453	289	58	123	10
166	36.27	0.46	3.03	50	12.68	1.21	11	48	13	40	275	20	398	263	46	96	5
165	36.88	0.58	3.72	158	7.53	1.56	11	52	15	51	319	16	353	313	49	89	11
163	37.64	0.51	3.69	156	13.77	1.36	9	58	14	49	371	20	368	277	58	104	8
160	39.17	0.44	3.36	213	27.82	1.18	9	47	15	36	592	16	204	255	30	40	6
157	40.54	0.62	4.81	203	10.72	1.46	14	74	13	57	637	18	220	349	29	65	12
154	41.91	0.66	4.70	198	12.73	1.44	20	79	13	57	740	20	314	343	31	60	11
151	43.28	0.61	4.62	195	11.37	1.45	12	79	9	55	575	23	362	332	44	97	14
150	43.74	0.25	1.64	69	17.60	1.07	9	42	9	27	664	13	188	219	28	60	<5
148	44.56	0.46	3.53	50	21.75	1.12	11	48	9	40	528	18	281	247	29	57	8
145	46.18	0.19	1.60	168	41.56	0.90	13	28	<5	17	650	10	128	114	18	33	<5
142	47.55	0.46	3.14	133	25.12	1.13	12	52	10	39	670	14	215	225	30	53	<5
139	48.98	0.14	1.63	172	43.74	1.28	7	23	<5	13	591	11	66	71	24	29	<5
136	50.29	0.37	3.35	142	29.84	1.11	6	78	6	36	767	19	186	183	38	59	7

TABLE A1 | **Continued.**

AC	Depth	TiO_2	Fe_2O_3	MnO	CaO	K_2O	Cu	Zn	As	Rb	Sr	Y	Zr	Ba	La	Ce	Pb
#	m	wt%	wt%	ppm	wt%	wt%	ppm	ppm	ppm	ppm	ppm	ppm	ppm	ppm	ppm	ppm	ppm
133	51.82	0.16	1.92	122	42.05	1.34	<5	33	6	17	578	11	130	89	11	40	<5
130	52.43	0.48	3.60	76	19.12	1.23	13	58	10	44	1043	15	186	183	35	56	8
129	52.73	0.44	3.32	50	24.43	0.98	15	53	10	39	1009	15	172	163	26	57	7
128	52.97	0.33	2.67	113	31.72	0.93	12	48	9	26	890	13	138	131	28	42	<5
126	53.64	0.17	1.56	100	41.51	0.82	10	26	<5	14	772	10	78	59	22	36	<5
124	54.25	0.38	3.08	130	27.60	0.94	10	51	9	33	933	13	178	158	30	51	8
122	54.89	0.19	1.90	81	39.52	1.32	10	32	<5	15	768	11	91	83	25	41	<5
121	55.17	0.45	4.31	91	22.25	1.25	10	68	9	47	903	15	185	207	30	59	9
118	55.93	0.49	4.70	100	20.27	1.40	13	84	12	50	817	15	217	237	30	58	9
116	56.54	0.43	4.75	101	27.31	1.33	9	56	10	48	758	13	159	186	25	58	6
114	57.15	0.78	6.35	268	9.31	1.80	25	106	14	74	591	18	226	415	26	44	15
112	57.61	0.52	8.20	50	21.25	1.90	12	122	10	78	658	13	150	203	16	53	9
110	58.03	0.50	4.02	85	20.71	1.32	14	69	12	49	1030	15	186	219	28	58	9
108	58.52	0.35	2.74	116	33.54	1.13	11	58	6	29	951	10	115	129	22	45	5
106	59.07	0.29	2.74	116	36.57	0.94	10	57	10	26	1001	16	85	124	36	47	<5
104	59.56	0.38	5.63	119	31.21	1.60	11	64	7	48	879	10	101	127	16	28	<5
103	59.74	0.68	6.77	144	14.47	1.67	18	100	10	67	823	13	163	312	26	48	13
101	60.35	0.75	6.25	263	9.64	2.03	16	111	10	75	607	18	190	407	13	71	14
100	60.59	0.81	7.17	305	12.35	2.38	21	137	10	90	507	19	185	442	32	51	<5
99	60.81	0.76	7.90	168	15.60	2.23	19	143	10	89	509	17	139	362	16	77	8
98	61.11	0.80	8.52	181	15.95	2.25	24	131	14	96	668	16	137	297	36	64	<5
97	61.36	0.20	7.37	50	39.29	1.34	8	48	9	55	679	9	26	57	19	42	<5
96	61.57	0.58	12.60	50	22.74	2.37	21	92	22	107	585	16	58	93	22	47	7
95	61.75	0.51	14.27	50	16.77	3.00	14	82	26	106	467	15	52	103	21	49	9
94	61.87	0.13	6.99	50	39.13	1.65	21	40	15	46	644	7	38	58	21	34	6
93	62.03	0.39	11.55	50	19.03	2.55	9	168	29	81	352	13	85	111	13	43	10
91	62.33	0.10	4.02	85	41.63	1.14	11	35	10	27	599	5	32	63	15	27	<5
89	62.73	0.34	4.63	98	31.28	1.33	8	63	12	43	341	12	102	155	21	52	7
87	63.09	0.22	4.02	170	39.50	1.09	9	44	11	29	457	13	137	115	28	58	<5
86	63.25	0.33	5.18	50	32.26	1.13	6	67	16	39	402	20	178	170	35	92	<5
84	63.55	0.29	4.16	176	37.29	1.04	9	37	19	31	416	15	155	148	25	53	<5
83	63.64	0.51	6.79	50	14.21	2.09	12	73	15	55	277	26	279	234	45	108	6
82	63.70	0.23	1.81	191	36.79	0.84	7	16	7	10	368	10	169	143	24	61	<5
80	64.10	0.17	1.50	159	32.66	0.56	17	16	<5	<10	342	8	85	111	18	35	<5
79	64.22	0.08	0.98	146	29.41	0.61	10	9	<5	<10	114	3	48	71	16	25	<5
78	64.31	0.20	1.65	244	33.98	0.81	8	10	<5	<10	224	10	145	94	21	41	9
77	64.50	0.19	30.05	50	1.45	0.96	40	19	300	16	52	3	60	86	<10	26	35
76	64.62	0.36	3.37	215	27.60	1.43	22	75	8	45	413	16	170	216	35	56	12
75	64.92	0.29	3.04	257	32.22	1.30	15	50	6	38	563	12	135	175	20	45	10
73	65.68	0.31	2.96	251	33.34	1.18	13	47	<5	37	620	11	107	174	33	48	8
71	66.60	0.45	3.33	212	25.46	1.53	8	53	7	51	544	19	233	311	28	69	5
70	67.06	0.63	4.85	206	10.41	2.05	11	76	9	72	341	22	331	436	31	75	6
69	67.51	0.69	5.16	219	10.17	2.03	15	84	9	79	386	21	283	415	30	69	11
67	68.43	0.68	5.38	228	10.03	2.06	17	80	8	75	386	20	315	419	39	84	14
65	69.49	0.66	5.10	217	9.01	1.98	18	90	7	79	383	22	273	451	29	75	13
63	69.89	0.71	5.25	223	10.19	1.88	23	95	8	79	430	18	246	396	35	75	13
61	70.35	0.46	3.33	212	23.09	1.32	8	55	5	49	468	25	351	304	43	102	11
59	70.87	0.60	5.60	237	22.79	1.86	12	66	10	54	516	18	229	281	35	68	15
57	71.48	0.52	4.01	255	19.60	1.80	12	67	9	61	482	19	271	368	38	79	7
56	71.72	0.49	3.35	213	21.49	1.55	9	55	6	55	472	18	284	321	33	73	9
55	71.93	0.63	4.28	182	13.79	1.76	13	83	7	67	445	23	322	387	45	88	13
53	72.39	0.62	4.53	192	14.79	1.77	16	88	8	67	487	20	300	366	40	66	10
51	73.00	0.62	4.23	179	14.09	1.83	13	77	8	64	449	24	329	399	52	84	11

TABLE A1 | **Continued.**

AC	Depth	TiO_2	Fe_2O_3	MnO	CaO	K_2O	Cu	Zn	As	Rb	Sr	Y	Zr	Ba	La	Ce	Pb
#	m	wt%	wt%	ppm	wt%	wt%	ppm	ppm	ppm	ppm	ppm	ppm	ppm	ppm	ppm	ppm	ppm
49	73.58	0.56	3.72	158	20.50	1.56	10	68	6	55	503	17	250	325	37	83	7
47	74.01	0.60	4.13	175	15.18	1.72	16	79	9	62	486	22	311	355	24	71	10
45	74.52	0.55	3.84	163	16.91	1.61	12	75	7	61	467	20	308	367	42	71	12
43	75.13	0.62	4.26	181	14.50	1.80	13	79	9	67	503	23	324	417	39	95	10
41	75.74	0.45	3.22	204	26.38	1.30	10	57	6	49	578	15	226	298	34	71	9
39	76.29	0.58	4.15	176	15.74	1.66	11	75	9	59	507	20	289	358	47	93	8
36	76.81	0.63	4.39	186	15.96	1.67	18	82	8	64	558	18	290	384	35	86	11
34	77.27	0.63	4.33	183	16.23	1.62	15	85	8	63	575	17	249	362	33	78	13
33	77.51	0.56	3.92	166	23.78	1.57	14	72	6	57	602	17	247	336	35	71	11
31	78.03	0.59	4.35	184	19.37	1.68	11	78	10	63	635	20	228	353	29	70	9
29	78.64	0.62	4.37	92	18.64	1.69	22	91	7	64	636	19	251	358	38	72	11
28	78.85	0.64	4.62	98	18.57	1.74	14	86	10	64	647	18	243	357	44	68	12
26	79.19	0.63	4.71	100	18.52	1.75	18	92	11	63	662	18	209	316	30	64	9
24	79.80	0.64	4.64	98	20.23	1.60	17	103	10	61	694	19	194	310	34	70	14
22	80.22	0.52	4.08	173	21.60	1.39	18	80	10	56	656	18	175	294	35	70	13
20	80.77	0.65	4.75	101	17.83	1.57	18	84	9	63	677	19	174	319	37	76	15
18	81.23	0.61	4.70	199	18.47	1.53	16	83	12	63	713	18	224	340	49	89	11
16	81.69	0.46	3.71	236	26.93	1.66	17	67	6	56	746	17	194	293	18	64	9
15	81.90	0.55	4.46	189	21.53	1.52	16	99	7	66	778	17	179	340	37	74	11
13	82.45	0.51	4.20	178	24.57	1.58	18	76	8	60	789	17	170	300	40	68	11
11	83.06	0.64	5.08	108	19.33	1.81	14	88	10	72	744	15	195	355	41	84	14
10	83.27	0.58	4.90	208	19.19	1.67	16	86	9	71	761	16	167	328	26	70	14
9	83.48	0.58	4.72	200	19.77	1.79	17	92	8	68	745	15	190	356	33	92	12
7	83.82	0.40	3.41	216	27.55	1.69	8	60	6	49	652	14	169	277	30	57	12
5	84.49	0.38	3.24	206	31.00	1.52	13	59	6	44	670	12	176	249	28	67	9
3	85.04	0.47	4.21	178	26.80	1.61	15	86	9	58	637	19	193	305	38	89	10
1	85.31	0.56	5.14	218	21.02	1.77	15	93	9	69	648	19	231	358	32	62	12

TABLE A2 | **Major and trace element composition of bulk samples from the Antioch Church core by wavelength-dispersive X-ray fluorescence spectrometry (WDS). All Fe is given as Fe_2O_3.; LOI is loss of ignition.**

AC	Depth	SiO_2	TiO_2	Al_2O_3	Fe_2O_3	MnO	MgO	CaO	Na_2O	K_2O	P_2O_5	LOI	Total
#	m	wt%	wt%	wt%	wt%	wt%	wt%	wt%	wt%	wt%	wt%	wt%	wt%
110	57.91	41.47	0.62	12.37	5.05	0.02	1.91	17.74	0.35	1.37	0.15	18.28	99.32
108	58.52	25.65	0.35	7.21	3.46	0.02	1.17	31.09	0.22	0.80	0.05	28.74	98.77
106	59.07	37.83	0.53	11.58	7.55	0.02	2.20	17.01	0.26	1.76	0.07	21.20	100.01
104	59.56	44.97	0.69	13.74	7.85	0.03	2.33	11.28	0.36	1.90	0.08	17.01	100.24
103	59.74	45.31	0.71	14.14	8.06	0.03	2.37	11.48	1.04	1.97	0.08	14.06	99.25
102	60.20	48.79	0.76	14.45	6.76	0.03	2.29	9.44	0.46	1.98	0.09	15.20	100.26
101	60.35	48.62	0.79	15.11	6.91	0.03	2.32	8.79	0.57	2.03	0.11	14.36	99.65
100	60.59	49.79	0.79	14.59	7.87	0.04	2.39	8.45	0.59	2.45	0.12	12.73	99.80
99	60.81	46.38	0.68	13.26	9.29	0.03	2.52	11.48	0.51	2.56	0.12	13.79	100.62
98	61.11	44.88	0.63	12.86	11.00	0.02	2.69	10.19	0.34	2.95	0.16	14.67	100.39
97	61.36	20.89	0.13	3.69	10.27	0.01	1.60	27.30	0.17	2.31	0.22	33.91	100.48
96	61.57	40.49	0.29	8.09	16.07	0.01	2.94	12.34	0.18	4.13	0.40	14.97	99.91
95	61.75	45.80	0.29	8.13	16.58	0.01	3.14	9.42	0.18	4.21	0.42	12.22	100.39
94	61.87	24.18	0.11	3.33	8.66	0.02	1.45	33.69	0.12	1.86	0.18	27.83	101.43
93	62.03	52.35	0.23	6.65	12.50	0.01	2.25	11.28	0.21	3.14	0.33	11.75	100.69
92	62.12	19.41	0.08	2.22	5.40	0.02	0.97	38.57	0.15	1.04	0.14	32.50	100.50
91	62.33	22.70	0.11	2.98	5.65	0.02	1.02	35.72	0.17	1.16	0.15	30.50	100.20
90	62.58	53.73	0.28	7.08	9.67	0.01	1.91	13.49	0.30	2.53	0.29	11.98	101.28
88	62.94	22.32	0.16	3.63	3.90	0.02	0.89	36.46	0.19	0.83	0.18	31.16	99.75
87	63.09	32.19	0.23	3.70	5.52	0.02	1.00	31.96	0.34	1.22	0.33	22.77	99.27
86	63.25	40.19	0.30	5.00	6.14	0.02	1.05	23.68	0.60	1.46	0.48	20.37	99.30
85	63.40	45.87	0.32	5.55	6.55	0.02	1.09	22.44	0.49	1.56	0.52	15.29	99.69
84	63.55	37.75	0.27	4.22	5.16	0.02	0.87	28.10	0.44	1.16	0.40	21.38	99.77
83	63.64	65.10	0.42	6.87	7.68	0.02	1.29	7.34	0.64	2.16	0.60	6.97	99.09
82	63.70	53.09	0.26	3.20	2.24	0.03	0.38	22.83	0.55	0.67	0.12	16.75	100.10
81	63.86	48.92	0.15	2.31	2.14	0.03	0.43	25.85	0.49	0.43	0.21	18.89	99.84
80	64.10	62.61	0.17	2.21	2.05	0.02	0.36	17.34	0.25	0.49	0.27	14.10	99.87
79	64.22	56.57	0.12	1.72	1.46	0.03	0.18	22.70	0.30	0.34	0.08	16.32	99.83
78	64.31	56.56	0.24	2.38	2.21	0.03	0.59	24.18	0.34	0.45	0.15	12.53	99.68
77B	64.47	53.71	0.06	1.09	20.96	0.01	0.07	0.28	0.20	0.26	0.03	21.84	98.51
77A	64.50	53.32	0.06	1.10	21.20	0.01	0.07	0.29	0.20	0.25	0.03	22.01	98.54
76	64.62	47.50	0.44	9.21	4.42	0.04	1.03	21.11	0.59	1.38	0.19	13.86	99.76
75	64.92	35.44	0.28	6.13	3.79	0.03	0.76	29.33	0.45	0.94	0.27	22.29	99.71
74	65.23	36.25	0.28	5.91	3.73	0.04	0.79	27.87	0.43	1.01	0.27	23.70	100.27
73	65.68	35.63	0.31	6.54	3.69	0.03	0.78	28.19	0.39	1.00	0.18	22.90	99.66
71	66.60	44.53	0.48	9.02	4.08	0.04	0.98	21.35	0.58	1.62	0.17	16.89	99.74
70	67.06	63.24	0.65	12.00	5.02	0.03	1.20	6.93	0.72	2.06	0.09	7.62	99.57
69	67.51	59.20	0.71	13.72	5.51	0.03	1.50	7.28	0.89	2.18	0.10	8.93	100.06

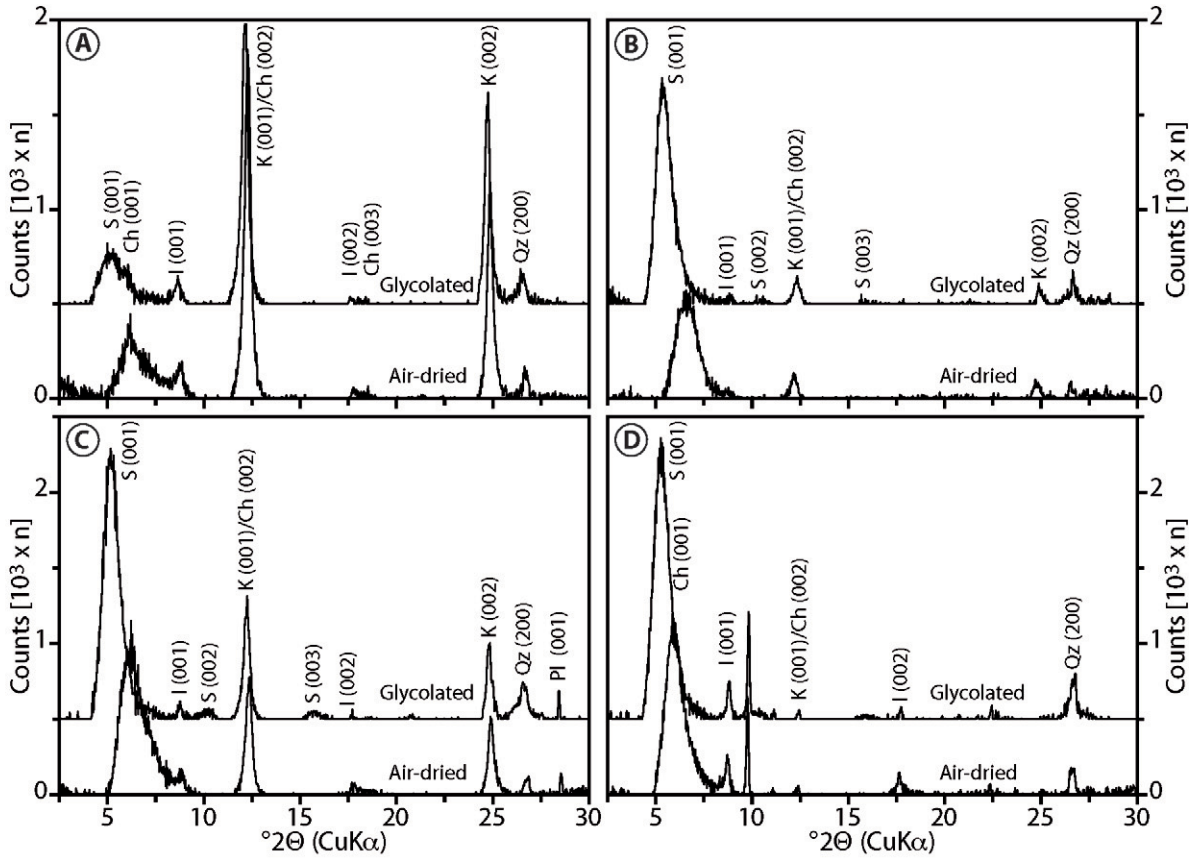

FIGURE A1 | **Representative X-ray diffraction patterns of the <2 µm fraction (air-dried and ethylene glycol-solvated) showing the three distinct clay mineral assemblages as well as the smectite-rich Clayton Basal Sands (see text for details). A) Prairie Bluff mudstone (Sample AC82). B) Clayton Basal Sands (AC82). C) Basal Pine Barren Member (AC119). D) McBryde Member (AC194).**